Development of a Trail Management Program

Final Report
December 2025

ctre
Center for Transportation
Research and Education

IOWA STATE UNIVERSITY
Institute for Transportation

Sponsored by
Des Moines Area Metropolitan
Planning Organization

About the Center for Transportation Research and Education

The mission of the Center for Transportation Research and Education (CTRE) at Iowa State University is to conduct basic and applied transportation research to help our partners improve safety, facilitate traffic operations, and enhance the management of infrastructure assets.

About the Institute for Transportation

The mission of the Institute for Transportation (InTrans) at Iowa State University is to save lives and improve economic vitality through discovery, research innovation, outreach, and the implementation of bold ideas.

Iowa State University Nondiscrimination Statement

Iowa State University does not discriminate on the basis of race, color, age, ethnicity, religion, national origin, pregnancy, sexual orientation, genetic information, sex, marital status, disability, or status as a U.S. Veteran. Inquiries regarding nondiscrimination policies may be directed to Office of Equal Opportunity, 2680 Beardshear Hall, 515 Morrill Road, Ames, Iowa 50011, telephone: 515-294-7612, email: eooffice@iastate.edu.

Disclaimer Notice

The contents of this report reflect the views of the authors, who are responsible for the facts and the accuracy of the information presented herein. The opinions, findings and conclusions expressed in this publication are those of the authors and not necessarily those of the sponsors.

The sponsors assume no liability for the contents or use of the information contained in this document. This report does not constitute a standard, specification, or regulation.

The sponsors do not endorse products or manufacturers. Trademarks or manufacturers' names appear in this report only because they are considered essential to the objective of the document.

Technical Report Documentation Page

1. Report No.	2. Government Accession No.	3. Recipient's Catalog No.

4. Title and Subtitle	5. Report Date
Development of a Trail Management Program	December 2025
	6. Performing Organization Code

7. Author(s)	8. Performing Organization Report No.
Inya Nlenanya, Zia Zihan, Yazan Alatoom, Abdallah Al-Hamdan, and Omar Smadi	

9. Performing Organization Name and Address	10. Work Unit No. (TRAIS)
Institute for Transportation Iowa State University 2711 South Loop Drive, Suite 4700 Ames, IA 50010-8664	11. Contract or Grant No.

12. Sponsoring Organization Name and Address	13. Type of Report and Period Covered
Des Moines Area Metropolitan Planning Organization 420 Watson Powell Jr Way #200 Des Moines, IA 50309	Final Report
	14. Sponsoring Agency Code

15. Supplementary Notes

16. Abstract

This report outlines the development of a comprehensive trail management program designed to improve the maintenance of paved trails in Central Iowa. Using the innovative Iowa Data Bike—a data collection tool developed and built by the Des Moines Area Metropolitan Planning Organization in 2017 that integrates an electric-assist bicycle with a smartphone and a GoPro camera—the program collected detailed data on trail surface roughness and overall conditions. The primary objectives were to establish a standardized metric for trail surface roughness, termed the Bike Roughness Index (BRI), and to develop an automated framework for surface distress evaluation using deep learning techniques.

The BRI was calculated using accelerometer data, while trail conditions were assessed through double integration and whole-body vibration analyses. Additionally, a Mask R-CNN model was trained to detect, classify, and segment various types of trail surface distress, enabling accurate and efficient condition assessments. The results demonstrate that the Iowa Data Bike is effective for rapid data collection and that the BRI is a reliable measure of surface roughness. The deep learning model successfully identified and quantified different distress types, which can significantly aid in maintenance planning.

This integrated approach supports proactive maintenance strategies, ensuring the safety and quality of recreational trails. Moreover, the report provides guidelines for optimal data collection, highlighting the potential for these methods to be refined and applied across diverse trail management contexts.

17. Key Words	18. Distribution Statement
Iowa Data Bike—surface distress—surface roughness—trail management program	No restrictions.

19. Security Classification (of this report)	20. Security Classification (of this page)	21. No. of Pages	22. Price
Unclassified.	Unclassified.	96	NA

Form DOT F 1700.7 (8-72) **Reproduction of completed page authorized**

DEVELOPMENT OF A TRAIL MANAGEMENT PROGRAM

Final Report
December 2025

Principal Investigator
Inya Nlenanya, Research Scientist
Institute for Transportation, Iowa State University

Research Assistant(s)
Zia U. A. Zihan, Yazan Ibrahim Alatoom, and Abdallah Al-Hamdan

Authors
Inya Nlenanya, Zia Zihan, Yazan Ibrahim Alatoom, Abdallah Al-Hamdan, and Omar Smadi

Sponsored by
Des Moines Area Metropolitan Planning Organization

A report from
Institute for Transportation
Iowa State University
2711 South Loop Drive, Suite 4700
Ames, IA 50010-8664
Phone: 515-294-8103 / Fax: 515-294-0467
https://intrans.iastate.edu

TABLE OF CONTENTS

ACKNOWLEDGMENTS xi
EXECUTIVE SUMMARY xiii
INTRODUCTION 1
OBJECTIVE 3
DATA BIKE SYSTEM 4
METHODOLOGY AND DATA COLLECTION 5
Data Collection Program 5
Vertical Motion Data from Smartphone Sensor 6
Vision Data from Camera Sensor 7
Reference Profiler 9
ESTIMATING TRAIL SURFACE ROUGHNESS 11
Surface Roughness Evaluation Using Smartphones 11
Roughness Estimation Based on Accelerometer Readings 13
RESULTS OF ROUGHNESS EVALUATION 17
VISION-BASED AUTOMATED CONDITION ASSESSMENT 21
Overview of Computer Vision Tasks for Distress Evaluation 21
Automated Trail Distress Identification Workflow 23
Trail Dataset for Automated Detection 24
Mask R-CNN Based Instance Segmentation Method 26
Model Training 27
Model Predictions 28
Model Limitations 33
Filtering Prediction Redundancy 35
SURFACE DISTRESS QUANTIFICATION 37
Scale Model Validation 40
NETWORK-LEVEL DEPLOYMENT 43
Integrating Automated Distress Evaluation Framework with Historical Data 44
Data Quality Assessment and Outlier Detection 48
Time-Series Assessment of Distress-Level Trail Condition 50
DATA COLLECTION GUIDELINES 54
Experimental Setup and Analysis 54
Established Guidelines 55
DTIMS IMPLEMENTATION METHODOLOGY FOR TRAIL MANAGEMENT 57
Data Integration and Asset Inventory 57
Condition Assessment and Performance Metrics 57
Performance Curve Development 58

Treatment Definition and Costing 59
Decision Trees and Trigger Logic 59
Scenario Modeling and Reporting 60
Summary 61

SUMMARY AND FINDINGS 62

REFERENCES 65

APPENDIX A. QUALITY CONTROL PLAN FOR TRAIL MANAGEMENT PROGRAM – DES MOINES METROPOLITAN PLANNING ORGANIZATION 69

A.1. Introduction 69
A.2. Trail Management Program Overview 69
A.3. QC Objectives and Strategy 70
A.4. Equipment Calibration and Setup 72
A.5. Data Collection Quality Control 74
A.6. Ground Reference and Validation 77
A.7. Automated Distress Detection QA 77
A.8. GIS and Data Management QA 78
A.9. Corrective Actions and Error Resolution 79
A.10. Training and Documentation 80
A.11. Reporting and Continuous Improvement 81

LIST OF FIGURES

Figure 1. Iowa data bike system 4
Figure 2. Workflow for trail condition assessment....5
Figure 3. Map location for the selected control sites....6
Figure 4. Control sites data collection 6
Figure 5. Acceleration data collected from smartphone accelerometer....7
Figure 6. Trail images captured by GoPro camera on the control sites....8
Figure 7. Walking profiler used as the reference profiler....9
Figure 8. Reference roughness measurements calculated using ProVAL software 10
Figure 9. Trail roughness evaluation using data bike method 13
Figure 10. RMSE values versus different section lengths using the double integration and whole-body vibrations methods 18
Figure 11. Comparison of BRI values (RMS method) for two runs in inverse and normal directions on different section IDs: demonstrating consistency and similarity in pavement roughness measurements 19
Figure 12. Comparison of BRI values (double integration method) for two runs in inverse and normal directions on different section IDs: demonstrating consistency and similarity in pavement roughness measurements....20
Figure 13. Computer vision tasks for distress evaluation....22
Figure 14. Workflow for automated trail distress identification....23
Figure 15. Proposed distress classes for trail surface 25
Figure 16. Distribution of trail distresses in the final dataset for training and validation sets 26
Figure 17. Mask R-CNN architecture....27
Figure 18. Model prediction evaluation....33
Figure 19. Instances showing model limitations....35
Figure 20. Comparison of model output before and after filtering algorithm application 36
Figure 21. Comparison of model output before and after filtering algorithm application 36
Figure 22. Tapes with known lengths placed on the trail segment for calibration 38
Figure 23. Illustration of the process to calculate the distance from the bottom of the image to the center of the bounding box....39
Figure 24. Scale for transverse cracking and T-joint....40
Figure 25. Scale for longitudinal cracking....40
Figure 26. Results from validation experiments for the scale model 41
Figure 27. Trail condition based on BRI 43
Figure 28. Distress data quantified from images for the trail network 45
Figure 29. ArcGIS-based automation tool for refining image frequency at the network level 47
Figure 30. Distribution of distress measurements before and after IQR-based outlier removal, showing 97.8% data retention with 1,204 outliers removed from the dataset....49
Figure 31. Example of time-series trail condition assessment for ParkID 2709 50
Figure 32. Distress progression over four years: ParkID 1045....51
Figure 33. Distress progression over four years: ParkID 1728....52
Figure 34. Image distribution along ParkID 1728 for 2020–2022....53
Figure 35. Geo-referenced images from the experimental program plotted in GIS environment....54

Figure 36. Trail treatment decision tree 60
Figure A.1. Temporal alignment of QA activities relative to the data collection cycle 71

LIST OF TABLES

Table 1. Detailed camera settings used for data collection....8
Table 2. Optimal hyperparameter settings for trail distress detection....28
Table 3. Number of images collected and filtered for the trail network....44
Table 4. Trail segments with available historical data....51
Table 5. Experimental data collection configurations and results....54
Table 6. BRI classification system for trail condition assessment....58
Table A.1. Detailed camera settings used for trail data collection....73

ACKNOWLEDGMENTS

The research team would like to thank the Des Moines Area Metropolitan Planning Organization for sponsoring this research. In addition, the research team would like to acknowledge Zhi Chen, Carl Saxon, and Ben Woeber for their valuable contributions during control site selection and data collection.

EXECUTIVE SUMMARY

This report outlines the development and implementation of an advanced trail management program designed to enhance the maintenance of paved trails in Central Iowa. Using the Iowa Data Bike—a data collection tool developed by the Des Moines Area Metropolitan Planning Organization in 2017 that integrates an electric-assist bicycle with a smartphone and a GoPro camera—the program collected comprehensive data on trail surface roughness and overall conditions.

The study had two primary objectives: (1) to establish a standardized metric for assessing trail surface roughness and (2) to develop an automated framework for evaluating surface distress using deep learning techniques. To achieve these goals, a novel metric—the Bike Roughness Index (BRI)—was developed based on accelerometer data from the smartphone. Additionally, trail surface conditions were analyzed using both double integration and whole-body vibration methods. Notably, the whole-body vibration method yielded higher accuracy for asphalt concrete trails, while the double integration approach proved more effective for portland cement concrete trails.

Complementing these methodologies, a Mask R-CNN deep learning model was developed to automate the detection and classification of surface distress, enabling a cost-effective trail condition assessment framework that requires minimal human intervention. This framework was further extended to include a distress quantification system that facilitates measurements that are closely aligned with in-field assessments. Additionally, the multi-step distress assessment framework was applied to network-level historical data from the Des Moines area, enabling a time-series analysis of distress data over a five-year period. This assessment demonstrated the capabilities of the automated system while also highlighting data quality challenges.

Key findings indicate that the Iowa Data Bike is a robust tool for rapid, detailed data collection. The BRI reliably quantifies trail surface roughness, and the Mask R-CNN model effectively supports automated, accurate assessments of surface distress. This integrated approach—combining smartphone-based roughness evaluation with deep learning-driven distress detection—facilitates proactive maintenance planning, thereby ensuring the safety and quality of recreational pathways in Central Iowa.

Furthermore, this report presents guidelines for optimal data collection practices and emphasizes the potential for further refinement and application of these methods in diverse trail management scenarios.

INTRODUCTION

Trail management is crucial for maintaining the quality and safety of recreational pathways, which significantly contribute to the quality of life in Central Iowa. The region boasts over 600 mi of shared-use trails that link urban centers with natural landscapes, offering residents and visitors accessible recreational opportunities. Effective trail management ensures that these pathways remain safe and enjoyable, which is essential as trails attract tourists and support local economies. Proper maintenance also helps in preserving the trails' structural integrity, preventing the need for costly repairs and extending their lifespan. Additionally, well-managed trails encourage outdoor activities, promoting public health and well-being (Des Moines Area MPO 2018).

The current method of trail condition assessment in Central Iowa involves a combination of field investigations and innovative data collection technologies. Assessment efforts are significantly enhanced by the Iowa Data Bike, a data collection tool developed by the Des Moines Area Metropolitan Planning Organization in 2017 that consists of an electric-assist bicycle equipped with an iPhone, a GoPro camera, and a Samsung Gear 360. The Iowa Data Bike collects detailed data on trial roughness and surface conditions, improving data collection efficiency and covering extensive trail networks quickly and accurately. This geo-located data helps local agencies prioritize maintenance tasks effectively. The comprehensive reports generated from this data guide maintenance priorities, ensuring that trails remain safe and enjoyable for users. This systematic approach aligns with long-term transportation planning goals, emphasizing the importance of managing existing infrastructure to maintain high-quality trail networks. By engaging volunteers in the data collection process, the initiative fosters community involvement and awareness, enhancing the overall impact on trail preservation and user satisfaction (Des Moines Area MPO 2019).

While the Iowa Data Bike has significantly enhanced the efficiency and comprehensiveness of trail condition assessments in Central Iowa, there are several areas where further improvements can be made. One potential improvement involves the integration of advanced computer vision models for automated distress evaluation. These models can analyze the geo-located photos captured by the Iowa Data Bike to identify and classify various types of pavement distress with greater accuracy and consistency. Additionally, developing an engineered metric for roughness evaluation that leverages accelerometer data can provide a more holistic and precise assessment of trail conditions. Implementing machine learning algorithms to predict future trail deterioration based on historical data can also aid in proactive maintenance planning. These improvements would not only streamline the assessment process but also provide more actionable insights for maintaining and improving the trail network.

In light of these considerations, this project aimed to develop an improved pavement condition assessment method for all paved trails within Central Iowa for use by the Des Moines Area Metropolitan Planning Organization (MPO), its member cities and counties, and partner organizations such as the Iowa Natural Heritage Foundation. Using the data collected by the Iowa Data Bike, this study establishes a reliable method for assessing trail surface roughness by developing a roughness metric engineered for smartphone sensor-based accelerometer data. Additionally, the study introduces an automated framework for evaluating and quantifying

surface distress using advanced computer vision models applied to imagery captured by the Iowa Data Bike, specifically by the GoPro camera, thereby eliminating the need for human intervention. The outcome of this study is expected to significantly aid practitioners in identifying triggers for maintenance and rehabilitation strategies, effectively improving the overall decision-making process.

OBJECTIVE

The goal of this study was to develop a comprehensive and systematic approach for assessing and maintaining the condition of paved trails in Central Iowa, utilizing advanced technologies and methodologies to enhance the decision-making process for trail management and maintenance. Key objectives included the following:

- Employ and evaluate the acquisition of network-level condition data for trails by the Iowa Data Bike
- Develop and validate a standardized metric for assessing trail surface roughness using smartphone sensor-based accelerometer data
- Develop an automated framework for surface distress evaluation and quantification using advanced computer vision models from imagery captured by a GoPro camera mounted on the Iowa Data Bike
- Utilize the roughness metric and automated distress evaluation tool to provide actionable insights to practitioners for identifying maintenance and rehabilitation triggers

IOWA DATA BIKE

In 2017, the Des Moines Area MPO developed and built the Iowa Data Bike to facilitate efficient data collection across its extensive trail network. The Iowa Data Bike reduces the need for field inspections for trail condition assessment because it can collect data on pedestrian infrastructure while traveling at a bicycle's speed. Initially, the system was developed to complement, rather than replace, comprehensive physical inspections.

The Iowa Data Bike comprises three major components: an iPhone, a GoPro camera, and a 360-degree camera, which are mounted on the back of the bike as shown in Figure 1. The iPhone is equipped with an accelerometer sensor. The SensorLog app, installed on the iPhone, captures the accelerometer data while the bike is ridden at cycling speed. A GoPro camera is mounted on the back of the bike and can capture continuous, geo-tagged imagery while the bike is ridden. Finally, to ensure a complete visual record, a 360-degree camera is mounted on the assembly to capture panoramic views of the trail and its surroundings.



Figure 1. Iowa Data Bike

METHODOLOGY AND DATA COLLECTION

The methodology for assessing trail conditions using the Iowa Data Bike involved a comprehensive approach to capture and analyze trail surface roughness and distress data, as illustrated in Figure 2. The Iowa Data Bike, equipped with an iPhone and a GoPro camera, traverses the trail network to collect vertical acceleration data and geo-referenced images. The iPhone's accelerometer records z-axis acceleration data, reflecting vertical motion, while the GoPro captures wide-angle images at 2-second intervals. This study focused on eight trail segments in Central Iowa, collecting comprehensive accelerometer and vision data. These data were processed and analyzed to develop a standardized roughness metric and an automated computer vision tool for detailed condition assessment of the trail network.

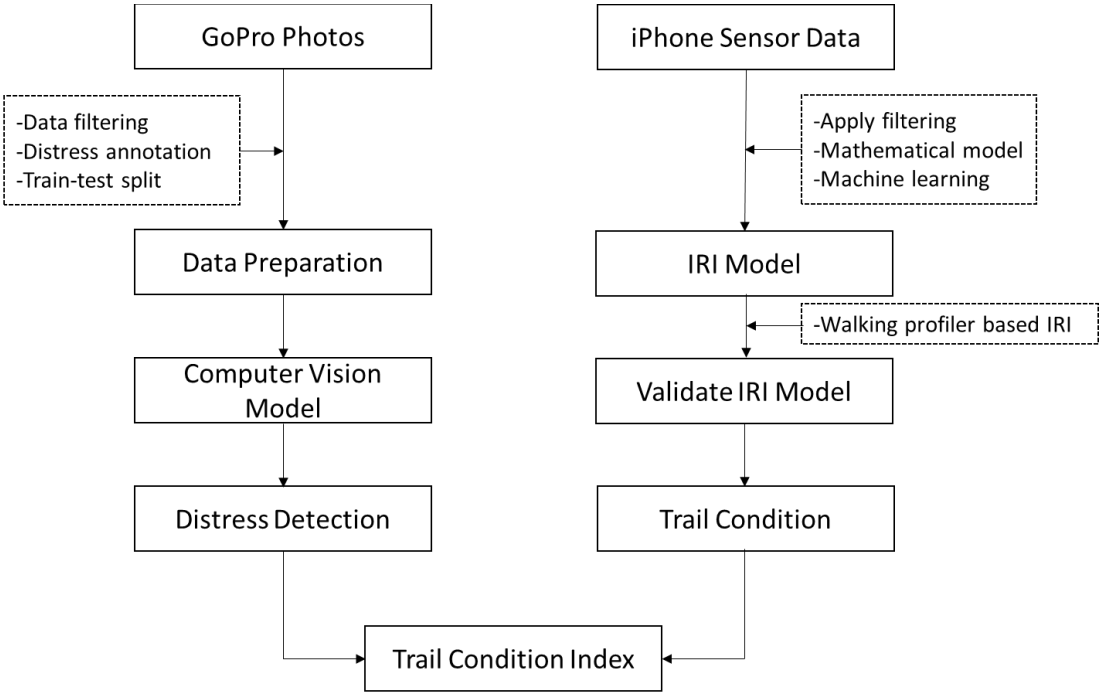


Figure 2. Workflow for trail condition assessment

Data Collection Program

The research methodology focused on eight trail segments in Central Iowa, each measuring approximately 0.30 mi (approximately 499 m) in length. These segments were divided into four asphalt concrete (AC) and four portland cement concrete (PCC) segments. The selection of these segments ensured adequate geographical spread, varying surface type and condition as mapped in Figure 3. Two types of data collection methods were employed: the smartphone-bicycle approach and the reference profiler for validating roughness indices, which in this case was the Australian Road Research Board (ARRB) walking profiler (Figure 4). A smartphone was mounted on a bicycle, as depicted in Figure 1, and four passes (two in each direction) were made on each segment to collect the following data:

- GPS data, including latitude, longitude, and speed
- Vibration data, comprising x, y, and z acceleration data
- Continuous geo-referenced photos covering the entire trail width

More details about the sensor specifications and configurations for collecting is presented in the subsequent sections.



Figure 3. Map location for the selected control sites



Figure 4. Control sites data collection

Vertical Motion Data from Smartphone Sensor

Employing the Iowa Data Bike (Des Moines Area MPO 2023), which is equipped with an iPhone smartphone, an evaluation of trail roughness was undertaken. The smartphone's onboard

sensors, including GPS for location tracking and accelerometer for measuring acceleration, played a pivotal role in data acquisition. Notably, the z-axis acceleration data from the accelerometer was utilized to characterize trail roughness, aligning with the vertical motion experienced during traversal. This data was synchronized with the corresponding latitude and longitude coordinates obtained from the GPS sensors, facilitating precise spatial mapping of roughness variations along the trail routes.

Smartphones equipped with a variety of sensors offer a wealth of data collection capabilities, extending beyond the commonly known GPS and accelerometer sensors. Additional sensors commonly found in smartphones include the gyroscope, which measures orientation and rotation rate, and the magnetometer, used for detecting the Earth's magnetic field. These sensors, alongside others such as the proximity sensor, ambient light sensor, barometer, temperature sensor, heart rate sensor, and fingerprint sensor, contribute to the device's multifunctionality and data-gathering potential. However, despite the availability of a diverse array of sensors, the evaluation of trail roughness focused primarily on a subset of sensor data. Specifically, the evaluation prioritized the z-axis acceleration data from the accelerometer and the latitude and longitude coordinates from the GPS sensors. This decision was driven by the unique requirements of assessing trail conditions, where precise spatial mapping of roughness variations was paramount. The z-axis acceleration data from the accelerometer played a pivotal role in characterizing trail roughness, as it directly reflects the vertical motion experienced during traversal. Trail roughness primarily impacts vertical movement, making the z-axis acceleration data particularly relevant for assessing unevenness and bumps along the route. Figure 5 shows a simplified illustration of how the accelerometer sensor collects the acceleration data.

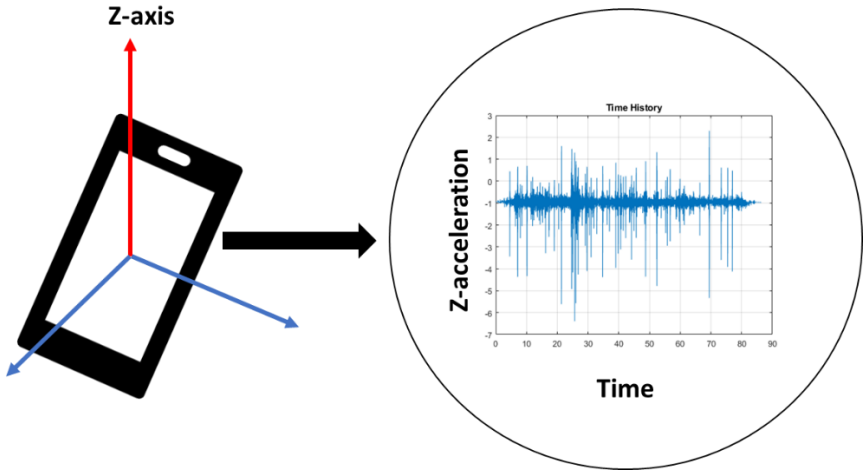


Figure 5. Acceleration data collected from smartphone accelerometer

Vision Data from Camera Sensor

For the purpose of collecting vision data, we employed the GoPro Hero 10 Black, which features a 23 MP camera equipped with a GP2 processor, enabling the collection of continuous geo-referenced photos. Table 1 shows the detailed configurations used for the collected vision data. The GoPro camera was strategically mounted on the back of the Iowa Data Bike, positioned at a

downward 45° angle to capture the full width of the trail surface. We set the camera to "wide angle" mode to capture the adjacent features of the trails. The images were captured in time-lapse mode at 2-second intervals. To ensure clarity in the captured images, the bike's speed was maintained between 7 to 8 mph. Figure 6 presents sample photos collected from the control sites.



Figure 6. Trail images captured by GoPro camera on the control sites

Table 1. Detailed camera settings used for data collection

Settings	GoPro Camera
Image Height	4000
Image Width	3000
Horizontal Resolution	72
Vertical Resolution	72
Color representation	sRGB
Camera maker	GoPro
Camera model	HERO5 Black
F-stop	f/2.8
Exposure time	1/1047 sec
ISO Speed	ISO-100
Exposure bias	0 step
Focal length	3 mm
Max aperture	2.97
Metering mode	Unknown
Flash mode	No flash function
35mm focal length	15
Contrast	Normal
Light Source	Unknown
Exposure program	Normal
Saturation	Normal
Sharpness	Hard
White balance	Auto
Digital zoom	1
EXIF version	0221

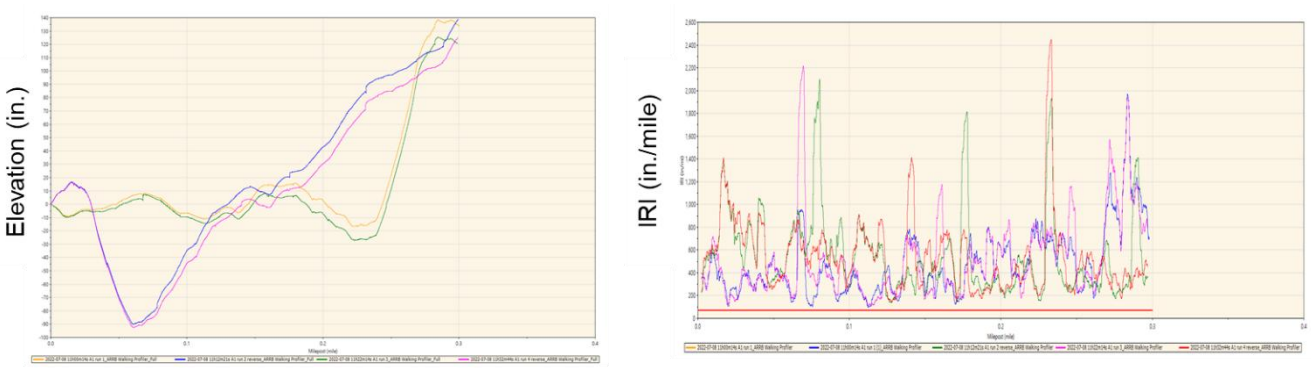
Reference Profiler

A walking profiler (shown in Figure 7) is typically used as a reference profiler to calibrate inertial profiler measurements of surface roughness. The accuracy of roughness measurements taken by a walking profiler is expected to range between 94% and 99%, and this varies based on the speed of walking during data collection (ARRB 2017). The walking profiler consists of an inclinometer, mounted on the measuring foot, which assesses either the gradient or the azimuth. The computer program computes a new reference height for each new step, which is updated by adding the relative height of the previous step. The relative height is determined based on the foot's inclination towards the vertical axis and the length of the section being measured. The device continuously records the pavement surface's longitudinal profile through a constantly lowered metal foot, recalculating and logging the cumulative height for each measuring section in reference to the starting point. An electronic walking profiler is capable of graphically displaying the results of profile measurements and automatically calculating the International Roughness Index (IRI) value.



Figure 7. Walking profiler used as the reference profiler

In the current study, the ProVAL software was used to calculate IRI by processing the elevation profile obtained for the trail surface. ProVAL generates a detailed report, including graphical representations of the raw elevation profile and the corresponding IRI values, as shown in Figure 8 for a sampled testing site.



a) Raw Elevation Profile

b) Reference Roughness Index

Figure 8. Reference roughness measurements calculated using ProVAL software

ESTIMATING TRAIL SURFACE ROUGHNESS

Surface roughness is a critical factor in the planning and maintenance of trail used for various forms of transportation, including bicycle (AASHTO 2012, Landis et al. 2004). It significantly affects the safety and comfort of cyclists (Bíl et al. 2015) and can lead to discomfort and reduced enjoyment for riders, potentially decreasing trail usage. IRI is a widely recognized metric used for assessing pavement quality, performance, and roughness (Al-Suleiman (Obaidat) and Alatoom 2022, Hosseini and Smadi 2021, Alatoom and Obaidat 2022). Initially developed for evaluating road surfaces, the IRI methodology, based on the quarter-car system (QCS), is adaptable to other types of surfaces, including trails. By simulating a vehicle traveling at a standardized speed, typically 49.71 mph (80 km/h), the vertical displacements of a simulated spring are measured to quantify surface roughness (Sayers 1986).

In this research, two different methods were employed to measure pavement roughness in terms of Bike Roughness Index (BRI) for the trails, namely *double integration* and *whole-body vibration*. The inclusion of these two methods allowed for a comparison and investigation of the most accurate approach to measure BRI. The subsequent sections outline the methodology used for data collection, as well as the development and evaluation of the proposed models.

Surface Roughness Evaluation Using Smartphones

In order to address the need for cost-effective and reasonably accurate methods to evaluate pavement roughness in a pavement network, numerous studies have been conducted to explore new techniques that are both low-cost and effective. Notably, there has been a significant focus on leveraging the accelerometer, gyroscope, and GPS sensors found in smartphones in recent years. Recent studies by Alatoom and Obaidat (2021), Janani et al. (2022), Sandamal and Pasindu (2022), Yang et al. (2022), and Zhang et al. (2022) have reported promising levels of accuracy when compared to other conventional methods for measuring IRI. These studies have concluded that the widespread use of smartphones among motorists presents intriguing possibilities for a faster and more affordable evaluation of pavement roughness (Yu et al. 2022).

One particularly notable and cutting-edge approach is the use of smartphones mounted on bicycles to measure IRI. These studies offer advantages over other smartphone-based methods as they can cover un-motorized lanes, such as trails, where automated pavement condition vehicles are not suitable. Two types of studies have emerged in this area. The first type focuses on evaluating pavement roughness for road pavements. For example, Shtayat et al. (2020) evaluated pavement roughness for a specific section of a local street in Australia using a smartphone mounted on a testing bicycle. The evaluation was based on vibration data collected from the z-axis of the smartphone's accelerometer sensor. However, the authors did not compare their results with any reference method, which is a notable disadvantage. Another study conducted by Cafiso et al. (2022) involved using smartphones placed on a bike and an e-scooter. The acceleration data collected from smartphones using the accelerometer was converted to RMS and then correlated with a reference IRI method, the Automatic Road Analyzer (ARA). Although outlier detection and speed adjustment methods were employed to minimize uncertainty in the IRI calculation, the correlations for both the bike and e-scooter were weak ($R^2 = 0.121$ and

0.057, respectively). This weak correlation could be attributed to the use of a relatively short measurement section of 10 m. Short sections are more susceptible to localized variations in the pavement surface, such as small bumps or dips, which can have a disproportionate impact on the measured IRI value. In contrast, using longer measurement sections can provide a more comprehensive and representative sample of the pavement surface, helping to minimize the impact of localized variations and provide a more accurate measurement of overall pavement roughness. Arora et al. (2021) examined the ability of a smartphone application called Roadroid, which is based on motorbike-mounted smartphones, to estimate IRI. However, both motorbikes provided weak correlations (R^2 = 0.104 and 0.028) when compared to reference IRI values. Using an android application like Roadroid without knowledge of how the IRI data were measured by the application does not facilitate the calibration process.

In the context of evaluating pavement roughness for trails and bicycle lanes, a second type of study has emerged. Titov and Schlegel (2019) developed a smartphone application that utilized the accelerometer and gyroscope sensors to classify cyclist ways using the K-Nearest Neighbor (K-NN) model. The classification criteria were established based on input from a group of cyclists, resulting in three classes: smooth, suitable, and unsuitable. Although the trained model demonstrated high precision (approximately 90%), the study did not discuss the calculation of IRI. Additionally, classifying cyclist ways into only three classes is insufficient for effective implementation of maintenance and rehabilitation plans. Another paper by Wage et al. (2020) focused on measuring two roughness indices, IRI and Dynamic Comfort Index (DCI), using acceleration data collected from a smartphone mounted on a bicycle. However, this study merely presented a methodology without validating the results against reference IRI data. As a result, the method cannot be considered valid until such validation is conducted.

Niska et al. (2022) aimed to assess the reliability of using smartphones on bicycles to evaluate riding comfort on cyclist ways. Acceleration data was collected using an accelerometer sensor and compared to IRI data obtained from a laser device, as well as survey data from cyclists regarding their perceived comfort. The authors claimed that IRI could not be used to assess the riding comfort of cyclist ways based on their results. However, they did not discuss the importance of calibrating the measured IRI from a new device against reference IRI before classifying it into comfort classes. Furthermore, they did not employ any filtering or cleaning methods to reduce uncertainty in the IRI data. These limitations raise concerns about the validity of their claim. Zang et al. (2018) developed a methodology for estimating pavement roughness in terms of IRI for trails using a combination of a smartphone mounted on a bicycle. Their methodology primarily involved converting acceleration data from the smartphone's accelerometer sensor into displacement values. The IRI was then calculated by dividing the accumulated displacement difference by the length of the road section. While their study demonstrated a high Pearson correlation (r = 0.893) compared to a professional laser profiler at a fixed bicycle speed of 15.5 km/h, their approach proved ineffective when applied to variable bicycle speeds, as maintaining a constant speed during the evaluation was challenging. Testing at variable speeds is a more realistic scenario in the field.

In summary, the aforementioned studies focused on evaluating pavement roughness for trails and bicycle lanes. While they introduced various methodologies and approaches, it is important for future research to address the limitations identified, such as validating results against reference

IRI data, calibrating measurements, employing data cleaning methods, and considering variable bicycle speeds in evaluations.

Roughness Estimation Based on Accelerometer Readings

Following data collection, rigorous analysis procedures were employed to enhance the quality of the acquired data. Initially, noise filters were applied to the acceleration data to remove the unwanted wavelengths and noise, ensuring data integrity critical for precise roughness estimation. Subsequently, signal processing techniques were utilized to convert the filtered acceleration data into a quantifiable roughness parameter, BRI. This involved extracting pertinent features from the acceleration signals indicative of trail condition, thereby furnishing a comprehensive measure of trail roughness.

The methodology used to evaluate trail roughness is presented in Figure 9. In the preprocessing step of the trail roughness evaluation, several key procedures were implemented to ensure the quality and relevance of the data collected. The first step involved the application of a High Pass Filter (HPF) based on the bike velocity. This filter was instrumental in isolating high-frequency components associated with variations in bike velocity, effectively separating them from the lower-frequency components related to trail roughness. Subsequently, data points corresponding to zero bike speed were removed based on GPS speed measurements. This process eliminated stationary periods where the bike was not in motion, ensuring that only data collected during active traversal of the trail was considered for roughness estimation. By filtering out stationary data points, the analysis focused exclusively on dynamic movement, enhancing the accuracy of the assessment. Following the filtering of velocity-related data, the trail was segmented based on GPS coordinates. Utilizing spatial information provided by the GPS sensors, the trail routes were delineated into distinct segments, each representing a specific section of the trail network. This segmentation facilitated a more granular analysis, allowing for the identification of roughness variations at different locations along the trail routes.

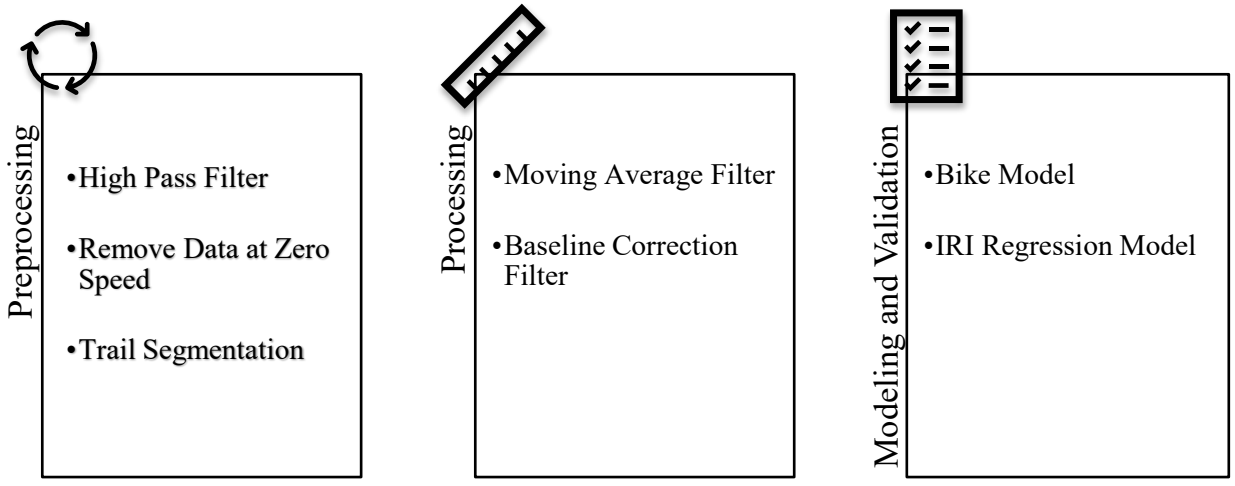


Figure 9. Trail roughness evaluation using the Iowa Data Bike

In the processing step of the trail roughness evaluation, several techniques were employed to refine the accelerometer data and derive meaningful insights into trail conditions. Double integration was utilized to convert the filtered accelerometer data into displacement measurements, offering a quantifiable representation of vertical movements experienced during trail traversal. This was complemented by the application of a moving average filter to smooth the displacement data, reducing noise and fluctuations caused by surface irregularities or sensor inaccuracies. Additionally, a baseline correction filter was implemented to mitigate systematic biases and ensure that the analysis focused solely on variations in trail roughness. These techniques collectively enhanced the accuracy and reliability of the data, facilitating a more comprehensive understanding of trail conditions and supporting informed decision-making for infrastructure maintenance and improvement efforts.

Following the processing step, the trail roughness evaluation underwent modeling and validation procedures to assess its accuracy and reliability. Validation was conducted using the walking profiler IRI. By comparing the roughness measurements obtained from the smartphone-based evaluation with those from the walking profiler IRI, a correlation was established, validating the effectiveness of the smartphone-based approach in assessing trail conditions.

Numerical Double Integration Method

In this approach, the collected vertical acceleration data was processed using a Butterworth high-pass filter of the second degree (Chou et al. 2020, Alatoom et al. 2024). This filtering step aimed eliminate unwanted wavelengths from the BRI data. The cutoff frequency of the filter was determined based on equation (1) as suggested by Chou et al. (2020). The resulting filtered data was then subjected to double integration to obtain displacement data based on equation (2) (Chou et al. 2020).

$$f = \frac{v}{\lambda} \tag{1}$$

$$D(n) = \iint_{t=0}^{t} a_z(t)\, dt^2 \tag{2}$$

To refine the displacement data, two additional filters were applied. The baseline correction filter, implemented using the BaselineRemoval 0.1.1 Python package, was used to remove trends caused by accumulated errors during the double integration process (Haque 2022). Additionally, a finite impulse response (FIR) moving average filter was employed to mitigate the impact of accelerometer noise on the displacement data (Chou et al. 2020).

After obtaining the displacement data, the BRI was calculated by summing the differences in vertical displacements and dividing by the segment length based on equation (3) (Chou et al. 2020). The segment length was determined using GPS data based on equation (4), which considers the latitude and longitude points of the segment (Chou et al. 2020).

$$BRI_s = \frac{\sum_{t=2}^{t} |D(t) - D(t+1)|}{L} \tag{3}$$

$$L = (2)(R)\arcsin\left(\sqrt{\sin^2\left(\frac{lat_2-lat_1}{2}\right) + \cos(lat_1)\cos(lat_2)\sin^2\left(\frac{long_2-long_1}{2}\right)}\right) \quad (4)$$

It is important to note that this approach assumes a rigid bicycle structure without any springs, which differs from a vehicle structure. Consequently, the computed vertical displacement of the bicycle is considered equivalent to the longitudinal profile (Zang et al. 2018).

Following the double integration method, a calibration step was performed to adjust the measured BRI values. The calibration coefficients, denoted asb_1 and b_2, were estimated to calibrate the measured BRI from the double integration method based on equation (5) (Chou et al. 2020).

$$BRI_{calibrated} = b_1(BRI_s) + b_2 \quad (5)$$

Whole-Body Vibration Method

The Whole-Body Vibration method follows ISO 2631-1, which serves as the standard for defining vibrations transmitted to the vehicle or bicycle body due to road conditions (ISO 2631-1, 1997). According to this standard, the root mean square (RMS) of vertical acceleration was calculated for each segment to assess pavement roughness (Ahlin and Granlund 2002). Equation (6) represents the calculation of RMS, where a_z (m/s^2) denotes the vertical acceleration in the time domain after applying a high-pass filter using Equation (1), and n represents the number of vertical acceleration data points collected for the segment.

$$RMS = \sqrt{\frac{\sum(a_z)^2}{n}} \quad (6)$$

Several researchers, including Ahlin and Granlund (2002), Zeng et al. (2015), Loprencipe et al. (2019), Chou et al. (2020), Alatoom and Obaidat (2022), and Cafiso et al. (2022), have explored the influence of speed on measured pavement roughness using the quarter golden car method. It has been observed that by considering the same whole-body vibration value of suspension relative velocity, equivalent vibration responses can be achieved for different velocities v_1 and v_2 (Sun et al. 2001, Múčka 2017). Consequently, the relationship between IRI threshold values and speed restrictions can be expressed as Equation (7) (Múčka 2017).

$$IRI_{v2} = (IRI_{v1})\left(\frac{v_1}{v_2}\right)^{0.5} \quad (7)$$

To incorporate the RMS parameter, Equation (7) is transformed according to Ahlin and Granlund (2002), resulting in Equation (8). This equation aims to remove the speed effect on pavement roughness by normalizing the RMS value with respect to speed (v) and a scaling factor (w).

$$\frac{RMS}{IRI} = 0.16\left(\frac{v}{80}\right)^{\frac{w-1}{2}} \quad (8)$$

For calibrating the measured IRI obtained from the walking profiler method and compensating for speed effects, Equation (9) is used. In this equation, the final calibrated BRI is calculated by considering the RMS value, the threshold speed (v_{th}) set at 80 km/h or 49.71 mph, the average speed on the segment (v), and calibration coefficients (b_1, b_2, and α). The calibration coefficients are estimated using the reference IRI data through the Levenberg–Marquardt algorithm (Levenberg 1944). The selection of 49.71 mph (80 km/h) as the speed threshold aligns with the default value used in the golden car model for IRI estimation (Uddin et al. 1990).

$$BRI_{calibrated} = b_1(RMS)\left(\frac{v_{th}}{v}\right)^{\alpha} + b_2 \quad (9)$$

RESULTS OF ROUGHNESS EVALUATION

The results of the proposed methods, namely double integration and whole-body vibration, along with their comparison, are presented in the following:

For the AC trails with 0.31 mi segments, regression models were developed using the double integration and whole-body vibration methods. Equation (10) represents the model derived from the double integration method, while Equation (11) represents the model derived from the whole -body vibration method. In Equation (10), BRI is measured in (in./mi), and RMS is measured in (m/s^2). The goodness of fit (R^2) and root mean square error (RMSE) for Equation (10) are 0.77 and 62.99, respectively. Equation (11) has an R^2 value of 0.90 and an RMSE value of 40.68. These results indicate that the whole-body vibration method outperforms the double integration method for AC trails.

$$BRI_{calibrated} = 0.926(BRI_s) - 209.204 \quad (10)$$

$$BRI_{calibrated} = 4.906(RMS)\left(\frac{49.71}{v}\right)^{1.882} + 94.267 \quad (11)$$

For the PCC trails with 0.31 mi segments, regression models were developed using the double integration and whole-body vibration methods. Equation (12) represents the model derived from the double integration method, while Equation (13) represents the model derived from the whole-body vibration method. In Equation (12), IRI and IRI_s are measured in (in./mi), and RMS is measured in (m/s^2). The R^2 and RMSE values for Equation (12) are 0.70 and 64.59, respectively. Equation (13) has an R^2 value of 0.62 and an RMSE value of 74.51. Interestingly, in contrast to the previous result, the double integration method performs better than the whole-body vibration method for PCC trails. This difference in performance could be attributed to the presence of transverse joints in PCC trails, which can affect the vertical vibrations of the whole body.

$$BRI_{calibrated} = 0.920(BRI_s) - 246.982 \quad (12)$$

$$BRI_{calibrated} = 20.785(RMS)\left(\frac{49.71}{v}\right)^{1.179} + 90.534 \quad (13)$$

Furthermore, the impact of section length on the accuracy of the proposed methods was investigated using different section lengths of 0.15, 0.1, and 0.05 mi. Figure 10 provides a summary of the results obtained from the whole-body vibration and double integration methods for AC and PCC trails with segment lengths ranging from 0.05 to 0.3 mi. The figure clearly demonstrates that as the section length decreases, the accuracy (RMSE) of the methods also decreases. This decrease in accuracy can be attributed to the inherent uncertainty in BRI measurements from run to run, particularly when the contact area between the bicycle tire and the pavement is relatively small compared to road vehicles (Jia et al. 2018). Additionally, GPS sensor errors can contribute to the reduced accuracy. On the other hand, when the section length is sufficiently long, the impact of these factors can be mitigated, as supported by the results. In

conclusion, both the double integration and whole-body vibration methods are not suitable for accurately estimating BRI for short section lengths.

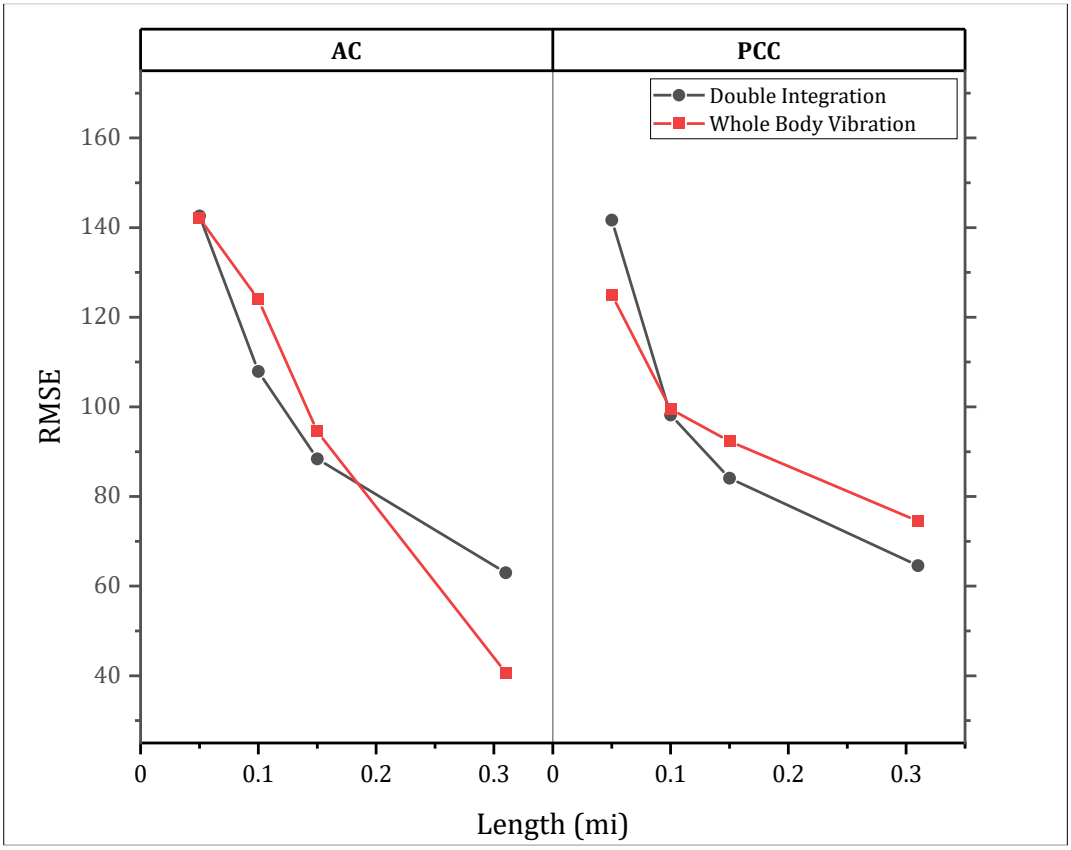


Figure 10. RMSE values versus different section lengths using the double integration and whole-body vibrations methods

Figure 11 presents the BRI values obtained using the RMS method for two runs in opposite directions (inverse and normal direction) on different section IDs. The y-axis represents the BRI values, which indicate the pavement roughness, while the x-axis represents the section IDs.The graph highlights the consistency of the BRI values produced by the model. The BRI values for each section ID, obtained from two runs in different directions, are close to each other in terms of their numerical values. This suggests that the BRI model generates consistent results regardless of the direction of measurement. The small difference between the BRI values in the inverse and normal directions indicates the reliability and robustness of the BRI model in producing consistent measurements.

Figure 12 illustrates the BRI values obtained using the double integration method for two runs in inverse and normal directions on different section IDs. The y-axis represents the BRI values, which indicate the pavement roughness, while the x-axis represents the section IDs. The graph showcases the consistency of the BRI values generated by the double integration method. The BRI values for each section ID, acquired from two runs in different directions, exhibit close proximity in terms of their numerical values. This consistency implies that the double integration

method consistently measures and estimates pavement roughness, regardless of the direction of measurement. The minimal disparity between the BRI values in the inverse and normal directions underscores the reliability and stability of the double integration method in producing consistent BRI measurements.

In conclusion, the findings from Figure 11 and Figure 12 suggest that the RMS method exhibits greater consistency in producing BRI values compared to the double integration method. The BRI values obtained from the RMS method for two runs in inverse and normal directions on different section IDs demonstrate close similarity, indicating a high level of consistency in pavement roughness measurements. On the other hand, while the double integration method also provides reasonably consistent BRI values, there appears to be slightly more variability between the runs in inverse and normal directions. Therefore, based on these observations, the RMS method can be considered as a more consistent approach for estimating BRI values, offering reliable and stable measurements of pavement roughness across different measurement directions and section IDs.

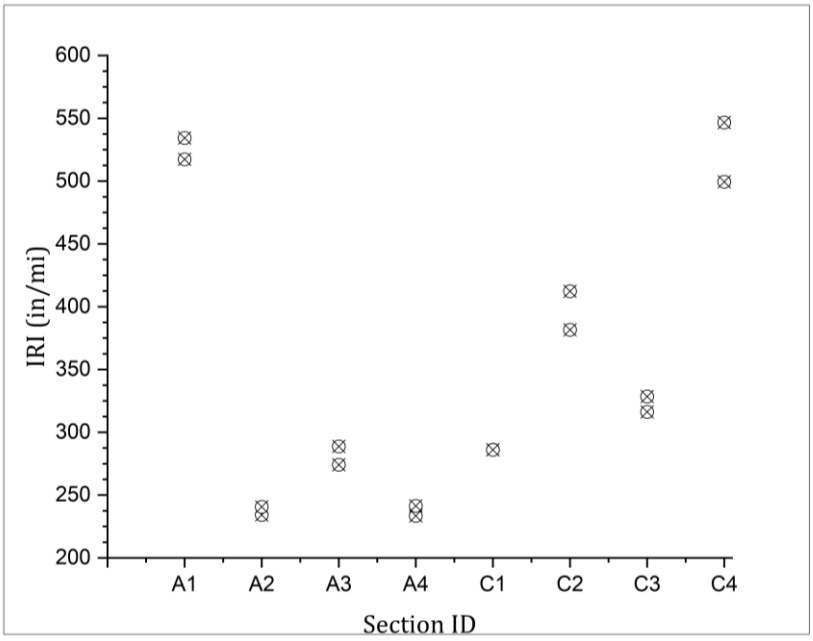


Figure 11. Comparison of BRI values (RMS method) for two runs in inverse and normal directions on different section IDs: demonstrating consistency and similarity in pavement roughness measurements

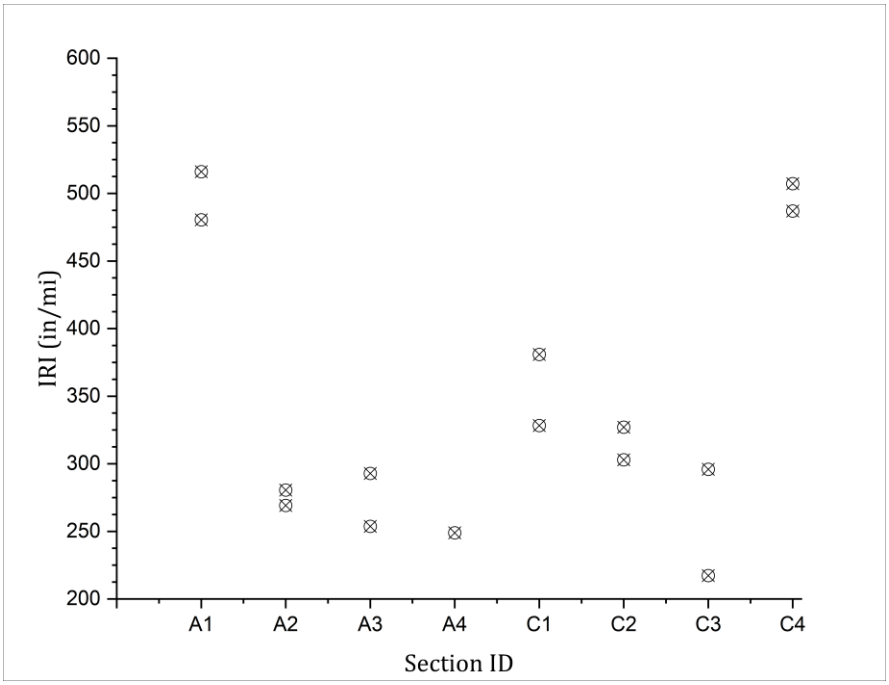


Figure 12. Comparison of BRI values (double integration method) for two runs in inverse and normal directions on different section IDs: demonstrating consistency and similarity in pavement roughness measurements

VISION-BASED AUTOMATED CONDITION ASSESSMENT

Automated condition assessment using deep learning in transportation infrastructure has gained significant attention in recent years due to the potential for more accurate and efficient evaluation processes. Deep learning methods, particularly in conjunction with image analysis techniques, have shown promise in advancing the assessment of infrastructure conditions (Ibragimov et al. 2024). Researchers have been exploring the application of deep learning, alongside computer vision and machine learning, to develop automated systems for evaluating conditions of the transportation infrastructure, aiming to make the assessment process faster, more cost-effective, and reliable (Qureshi et al. 2022). The integration of deep learning algorithms has been demonstrated to enhance the reliability of results in the analysis of sustainable operation in transport infrastructure projects under government regulation, suggesting the potential for deep learning to supplement future infrastructure analysis processes (Ma et al. 2021).

Moreover, the utilization of deep learning in conjunction with machine learning has been instrumental in automatically assessing damage in infrastructure, particularly in scenarios like flash flooding, where identifying damaged critical infrastructure can be challenging due to distinct appearances and limited training data (Sellami and Rhinane 2024). In the context of tunnel inspections, deep-learning methods, especially convolutional neural networks (CNNs), have shown promise in automatically detecting cracks on concrete surfaces and quantifying their characteristics, such as length and width, showcasing the potential for deep learning to enhance infrastructure assessment processes (Sjölander et al. 2023). Additionally, innovative approaches using deep learning and big data analytics have been proposed for infrastructure prioritization, showcasing the potential for advanced technologies to optimize decision-making processes in infrastructure management (Uwizera et al. 2022)

Overall, the synthesis of these references underscores the growing significance of deep learning in automated condition assessment across various domains of transportation infrastructure management. The studies highlight the potential of computer vision to enhance the accuracy, efficiency, and reliability of assessment processes, paving the way for more advanced and data-driven approaches to infrastructure evaluation.

Overview of Computer Vision Tasks for Distress Evaluation

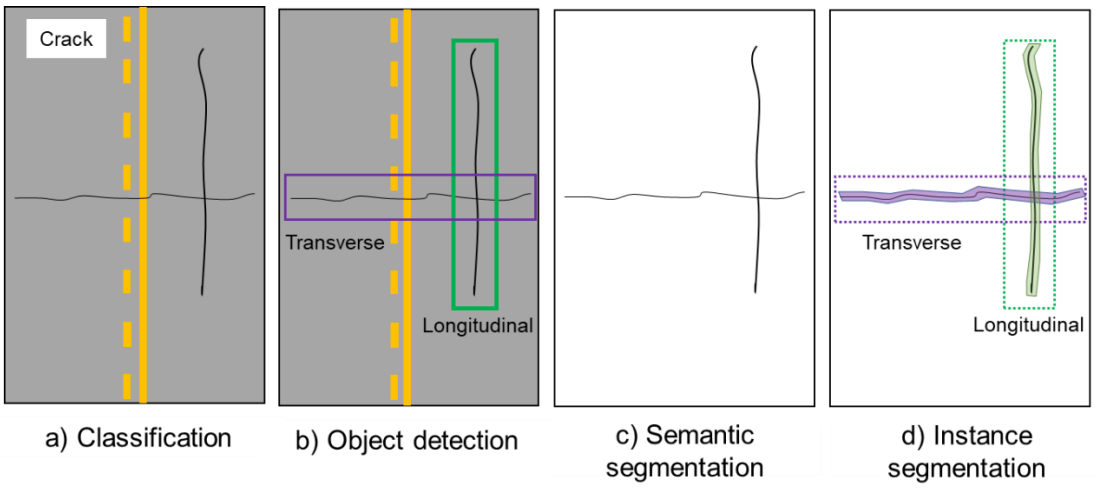
Researchers have utilized a range of traditional shallow and advanced deep learning algorithms on vision data to effectively extract distress attributes. Traditional or shallow algorithms for distress evaluation have been extensively studied. Commonly used techniques include thresholding, filtering, edge detection, wavelet transform, Hough transform, and support vector machine (SVM) (Hoang 2018, Mathavan et al. 2017). Despite their widespread application, these algorithms face challenges such as high computational demands and limited feasibility for production-level distress detection, as they are often tailored to specific scenarios (Ghosh and Smadi 2021).

In recent years, deep learning has become immensely popular, addressing many of the limitations associated with shallow algorithms. Unlike shallow methods, deep learning

algorithms can autonomously learn and extract feature maps from input images to localize, classify, or segment surface distresses (Hsieh and Tsai 2020). As a result, deep learning has become the state-of-the-art approach for distress detection. The following subsections briefly outline the tasks performed by deep learning models and their effectiveness in automating the distress evaluation process.

Initial efforts in vision-based pavement evaluation utilized Convolutional Neural Networks (CNNs) for image classification, which effectively classified 2-D pixel grids(Yamashita et al. 2018). However, this approach was limited as it could assign only a single class to an image, even if multiple distress types were present; see Figure 13(a). To address this limitation, advancements in deep learning have introduced object detection methods that detect and localize multiple classes within a single image. As shown in Figure 13(b), object detection models use bounding boxes to identify, localize, and classify distresses, thus these models have significantly enhanced the automation of pavement management. Nevertheless, object detection faces limitations: it cannot measure distress severity or exact crack widths, accurately represent curved shapes, or estimate the area of complex distresses like alligator cracking.

To overcome these limitations, semantic segmentation and instance segmentation techniques have been employed in pavement distress detection. Semantic segmentation assigns labels to each pixel in an image, enabling detailed distress shape detection, but it does not differentiate between distress classes; see Figure 13(c). Various deep learning methods, such as encoder-decoder models and GANs (Mei and Gül 2020), have been used with some success. Instance segmentation combines object detection and segmentation, allowing for both localization and per-pixel classification as shown in Figure 13(d). The Mask R-CNN method, a notable advancement, classifies and generates masks for detected objects (Zihan et al. 2023).



Zihan et al. 2023

Figure 13. Computer vision tasks for distress evaluation

Automated Trail Distress Identification Workflow

Figure 14 outlines a comprehensive workflow for trail distress assessment using deep learning techniques, starting from data collection to distress mapping. Initially, GoPro cameras capture trail photos, which are then annotated to label different types of distresses. These annotated images are converted into the COCO format, facilitating efficient dataset preparation. The dataset is split into training, validation, and testing subsets, each serving a specific purpose in the model development process. The training set is used to train the deep learning models, the validation set helps in tuning model parameters, and the test set evaluates the model's performance.

Model development begins with selecting the most suitable deep learning architecture, followed by hyper-parameter optimization to fine-tune the learning process. The model is then trained on the training dataset using optimized parameters. Post-training, the model's performance is assessed based on criteria such as precision, recall, F1-score. Once the model meets these assessment criteria, it performs inference on new, unannotated images to detect and classify trail distresses. The detected distresses are then mapped onto a trail map, providing a spatial representation that aids in targeted maintenance and management. This structured workflow ensures a robust, accurate, and reliable approach to trail distress assessment using deep learning.

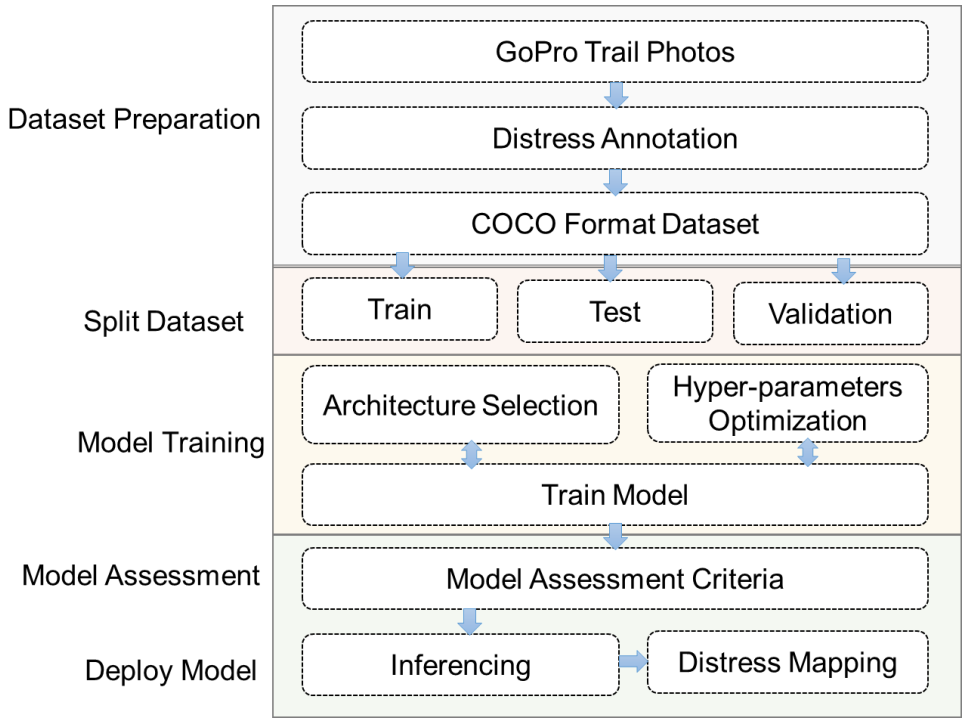


Figure 14. Workflow for automated trail distress identification

Trail Dataset for Automated Detection

This study identified and proposed eight types of trail surface distresses based on network-level imagery. These distresses were manually annotated to develop a comprehensive dataset, which was then used to train and validate a computer vision tool for the automated detection, classification, and segmentation of these distresses.

Proposed Trail Distresses for Automated Detection

For trail surfaces, no specific guidelines have been found in the literature regarding the distresses that need to be identified. Therefore, this study proposed eight types of distresses based on observations from screening network-level imagery captured by the Iowa Data Bike. These proposed distress types are as follows: (1) interconnected cracking, (2) longitudinal cracking, (3) sealed longitudinal cracking, (4) transverse cracking, (5) transverse joints, (6) spalling, (7) potholes, and (8) patching. The characteristics of most of these distresses are widely recognized within the pavement management community. However, for trail surfaces, these distresses can be defined as follows and their appearance have been demonstrated in Figure 15:

- *Interconnected Cracking*: These are instances where multiple longitudinal cracks intersect with each other, forming a network of cracks that typically indicate severe structural failure.
- *Longitudinal Cracking*: Cracks that run parallel to the trail's longitudinal direction
- *Sealed Longitudinal Cracking*: Longitudinal cracks that have been filled or sealed to prevent water infiltration and further deterioration.
- *Transverse Cracking*: Cracks that extend perpendicular to the trail's longitudinal direction, usually resulting from thermal expansion and contraction of the surface.
- *Transverse Joints*: These are intentional separations in the concrete trail surface, designed to control cracking and manage expansion and contraction.
- *Spalling*: The breaking, chipping, or fraying of the pavement surface, often occurring near joints on the concrete surface.
- *Potholes*: Bowl-shaped depressions in the trail surface caused by localized structural failures, often due to water infiltration and loading.
- *Patching*: Areas where the trail has been repaired by placing new material over damaged sections to restore functionality and smoothness.

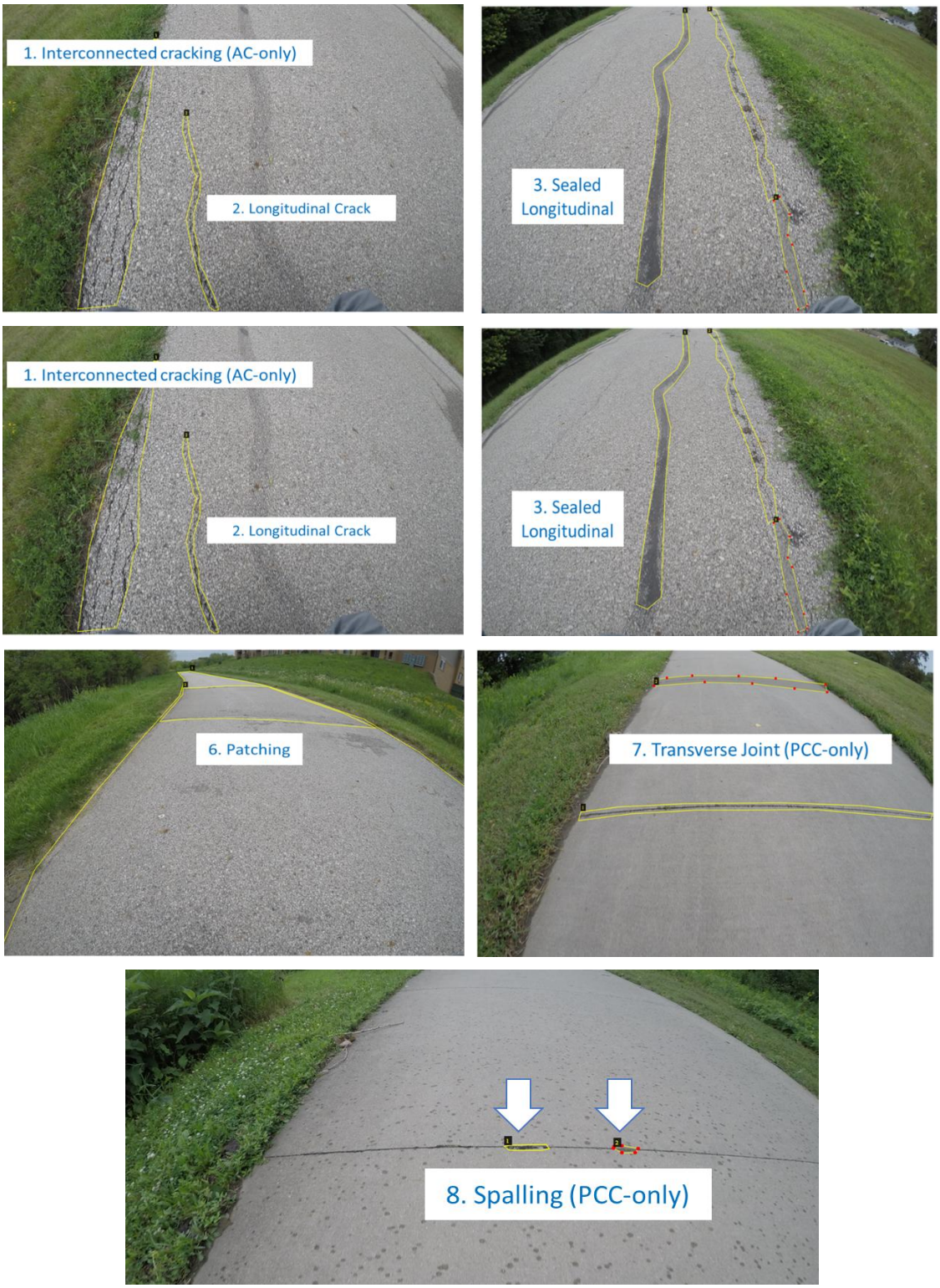


Figure 15. Proposed distress classes for trail surface

Distress Annotation for Automated Detection System

A critical step in preparing a dataset for training a computer vision model is the precise labeling or annotation of the objects to be identified. Training the Mask R-CNN model required precise polygonal annotations of these distress classes. These annotations were manually created within the training dataset to serve as input for the Mask R-CNN model.

The dataset was divided into two parts: 70% of the images were randomly selected for training, while the remaining 30% were used for model validation. Polygons were used to annotate the distresses using the VGG Image Annotation (VIA) tool, with the annotations saved in a JSON (JavaScript Object Notation) file. Due to the imbalance in the number of certain distress types, data augmentation was performed by rotating each image between -15° and +15° and applying a greyscale filter to 25% of the training images. No augmentation was performed on the validation set to maintain its independence from the training set. The annotations were formatted to suit the specific models used in this study. Figure 16 shows the number of instances from the final dataset for each class of distress, separately used for training and validation of the model.

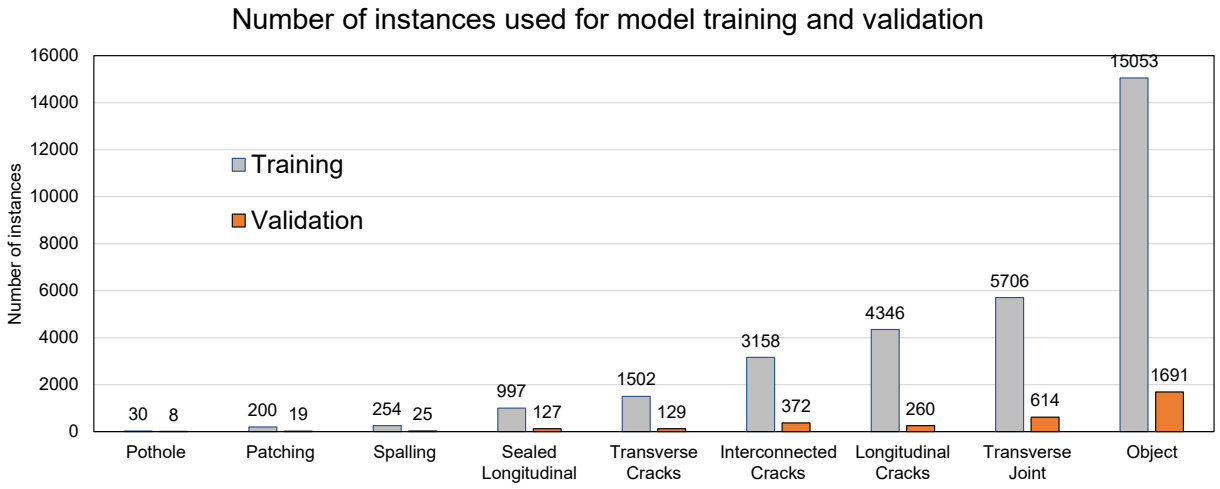


Figure 16. Distribution of trail distresses in the final dataset for training and validation sets

Mask R-CNN Based Instance Segmentation Method

The instance segmentation module of Mask R-CNN is the latest extension to the Faster R-CNN object detection algorithm. The framework is dependent on the open-source libraries of Keras and Tensorflow and consists of four major modules as the following (He et al. 2017):

- **Backbone**: It serves as a feature extractor from the input images. Typical backbone architectures are standard CNNs such as ResNet50, ResNet101, VGG16 etc. and may further be improved using Feature Pyramid Network (FPN). Lower and higher-level features are separately extracted by the different layers of the backbone architecture. This study uses ResNet101 with FPN as the backbone architecture.

- **Region Proposal Network (RPN)**: RPN, another lightweight network, generates sliding windows to scan over the feature map generated by the backbone architecture. RPN scans over the regions, also known as anchors, to find out the potential areas with object in it and generates two outputs: anchor class and bounding box refinement. The top anchors with higher foreground anchors predicted by RPN are subjected to refinement of their location and size. To improve RPN's performance, different hyperparameters such as RPN ratios, scales, stride, and threshold for non-maximum suppression (NMS) can be fine-tuned.
- **ROI Classifier and Box Regressor**: In this stage, the top anchors from RPN predictions are subjected to classification based on ROIAlign, which samples the feature map at different locations and applies a bilinear interpolation. Afterward, bounding box refinement is conducted similar to the previous stage to further refine the bounding box sizes and location. Lastly, a fully connected layer detects and classifies the detected distresses.
- **Segmentation Masks**: Until this stage, the method can be regarded as a Faster R-CNN algorithm for object detection and classification. The positive regions within the bounding box predicted by the ROI classifier are masked with a resolution of 28*28. The accuracy of the generated masks is calculated then by computing the loss from the ground-truth masks.

Figure 17 shows the schematic of the Mask R-CNN architecture adapted based on (Attard et al. 2019, Podder et al. 2021):

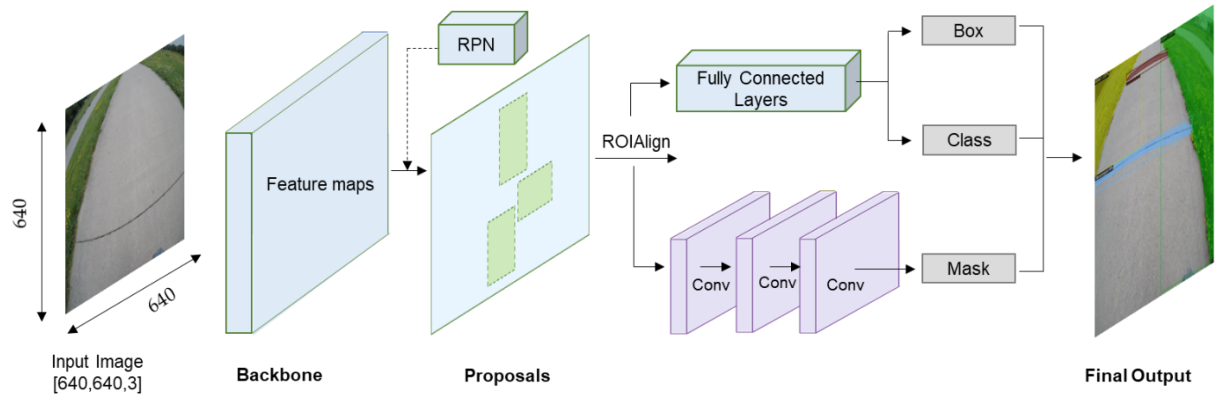


Figure 17. Mask R-CNN architecture

Model Training

The Mask R-CNN architecture was trained in a Google Colaboratory environment with an NVIDIA Tesla T4 GPU. The Detectron2 framework was employed for training and validating the Mask R-CNN models, as it is widely used for its ability to support various model configurations and backbone networks. Initially, different model backbones were trained for 50,000 iterations to determine the most effective architecture. During each iteration, the model calculated the loss function, quantifying the difference between the model's predictions and the ground truth. This loss was minimized using a stochastic gradient descent (SGD) optimizer, which iteratively updated the model parameters to reduce the loss. The training process utilized specific hyperparameter settings to optimize the model performance. These hyperparameters are detailed in Table 2 and play a crucial role in influencing the training dynamics and overall performance of the model.

- The learning rate determines the size of the steps taken during the optimization process. A well-chosen learning rate can accelerate convergence to the optimal solution, while a rate too high can cause overshooting and instability, and a rate too low can result in slow convergence and getting fixed in local minima. The optimal *learning rate* during model training for trail dataset was found at 0.001.
- The *optimizer* used was stochastic gradient descent (SGD), which updates the model parameters in the direction of the greatest decrease in loss. The momentum parameter, set at 0.9, helps accelerate SGD in the relevant direction and dampens oscillations, leading to faster convergence and more stable updates.
- *Weight decay*, is a regularization technique that penalizes large weights to prevent overfitting, improving the generalization of the model. A non-zero weight decay encourages the model to learn simpler and more robust features.
- The *Intersection over Union (IoU)* training threshold, set at 0.5, determines the threshold for deciding positive and negative samples during training. A higher IoU threshold can make the training stricter, potentially leading to more accurate detections, but it might also reduce the number of positive samples and make the training more difficult.
- Th *batch size* of 2 influences the number of training examples used in one iteration of training. A smaller batch size, such as 2, allows for more frequent updates and can lead to better generalization, though it can make the training noisier and slower.

These carefully selected hyperparameters collectively ensure the model achieves optimal performance in trail distress detection by balancing the speed of convergence, the ability to generalize, and the stability of the training process.

Table 2. Optimal hyperparameter settings for trail distress detection

Mask R-CNN Hyperparameters	
Learning rate	0.001
Optimizer	SGD
Momentum	0.9
Weight Decay	0.0001
IoU training threshold	0.5
Batch size	2

Model Predictions

The trail distress detection model exhibits robust performance in detecting trail surface distresses across various conditions, as demonstrated by the provided images in Figure 18. On AC surfaces, the model accurately identifies trails in good condition and effectively detects potholes, multiple longitudinal cracks, and far-located transverse cracks. It also performs well in heavily cracked areas, accurately distinguishing and identifying overlapping cracks. On concrete surfaces, the model reliably identifies longitudinal cracks and transverse joints. The model maintains its accuracy in challenging scenarios, such as skewed images, where it successfully detects transverse joints, and shadowed images, where it identifies both transverse joints and spalling. Additionally, the model shows a strong capacity for detecting critical distress types like

interconnected cracks. These results underscore the model's potential for practical applications in trail distress assessment, highlighting its reliability and versatility in various real-world conditions.

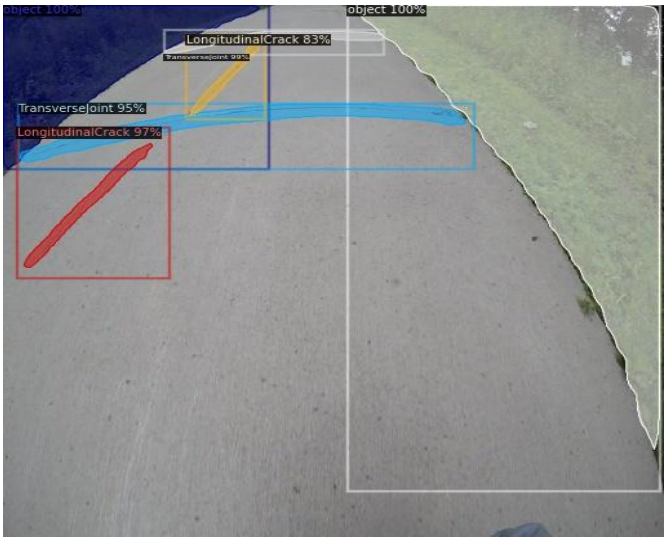
Performed robustly on concrete surfaces:

- Identifying Transverse Joints



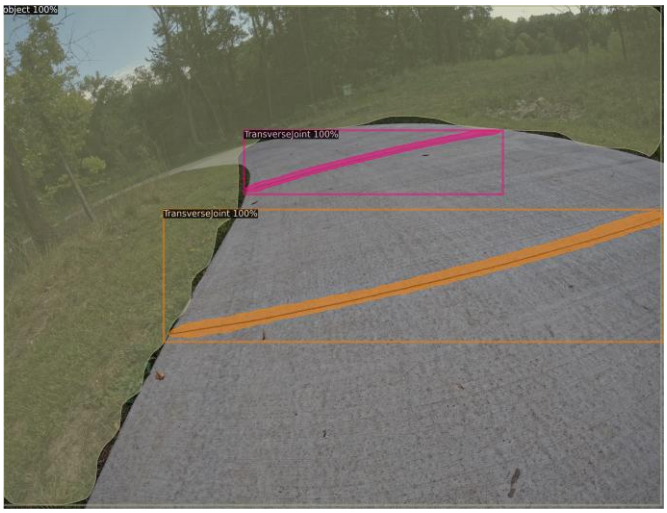
Performed robustly on concrete surfaces:

- Identifying Longitudinal cracks and Transverse Joints



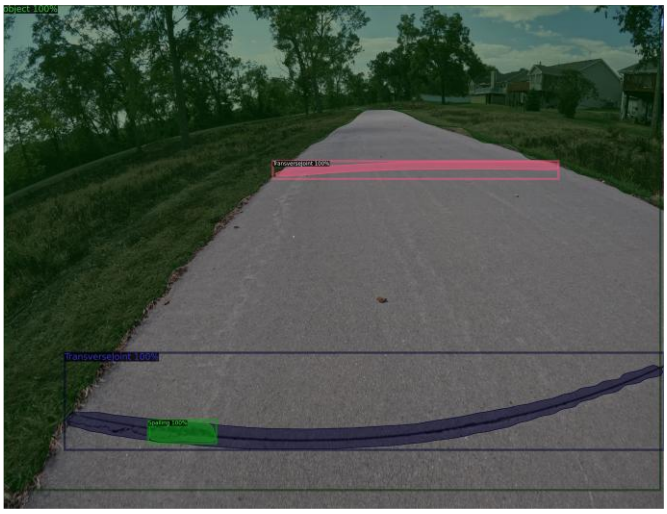
Performed well on skewed images:

- Transverse Joints appearing skewed



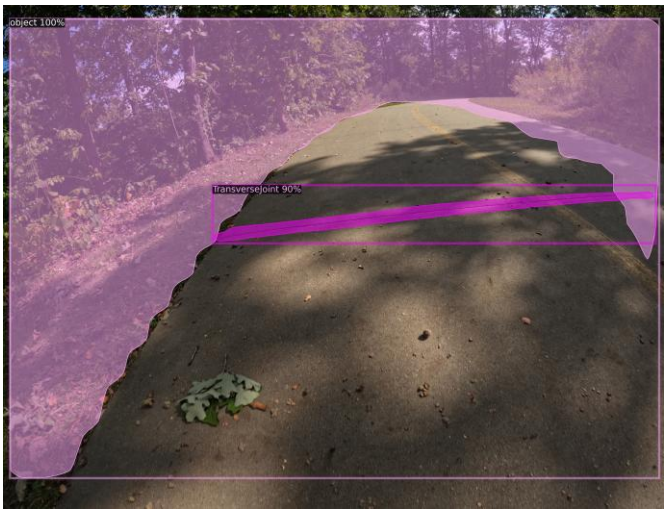
Performance on smaller sized distress:

- Spalling detected on Transverse Joint



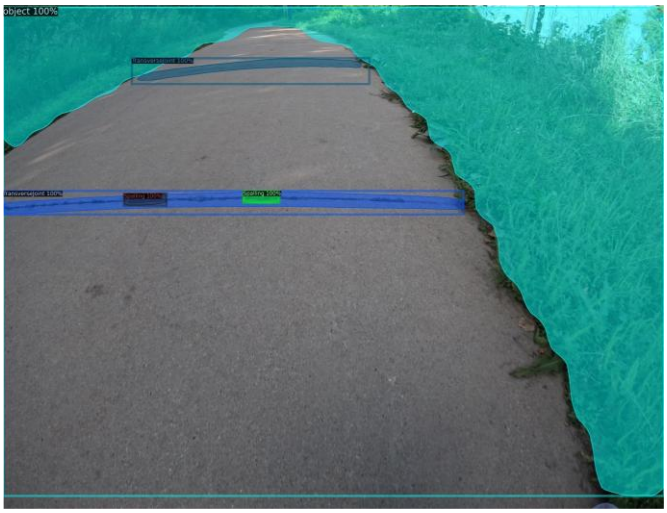
Performed well on shadowed images:

- Transverse Joints detected



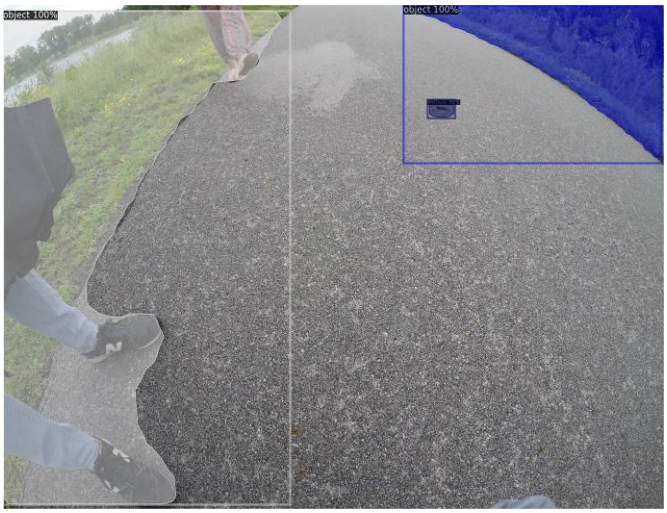
Performed well on shadowed images:

- Spalling detected on Transverse Joint



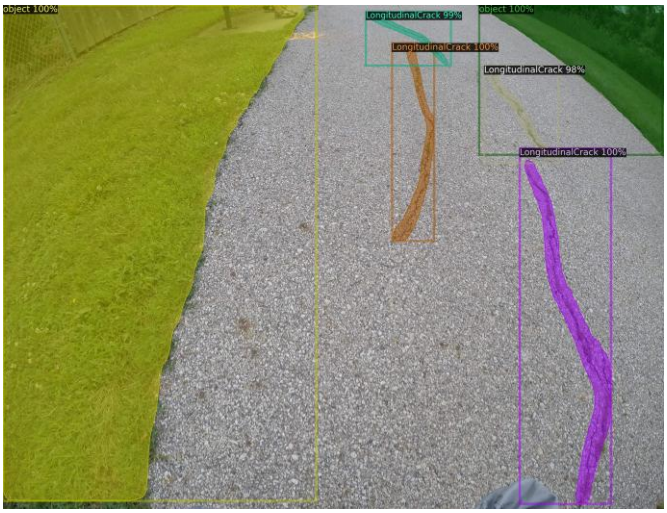
Model performance on AC surface:

- Pothole detected



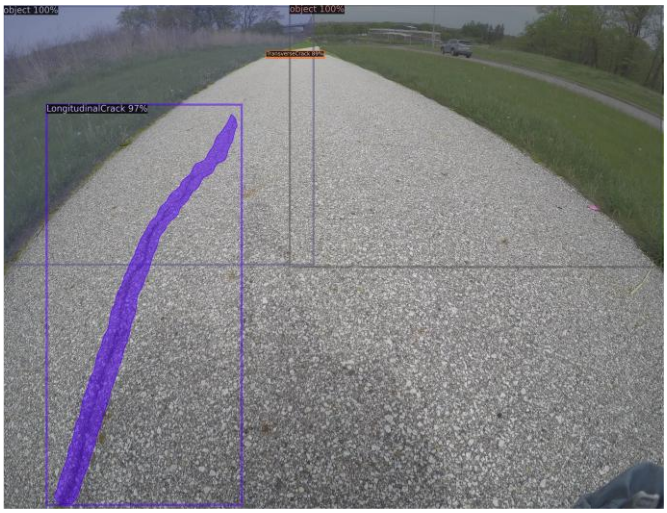
Model performance on AC surface:

- Multiple longitudinal cracks detected



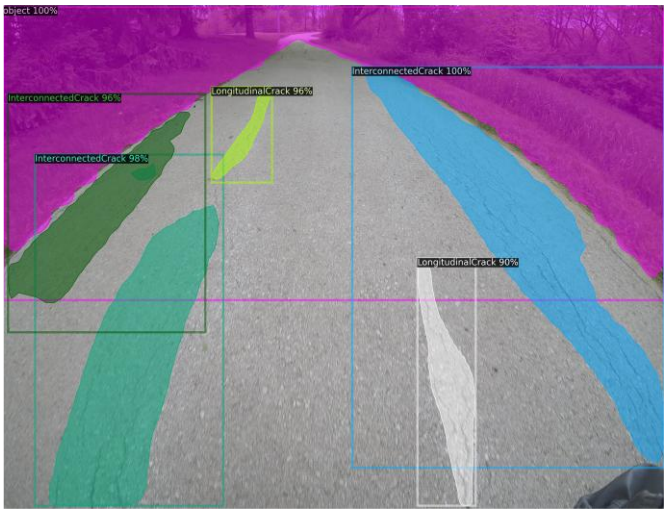
Model performance on AC surface:

- Detection of far located transverse cracks



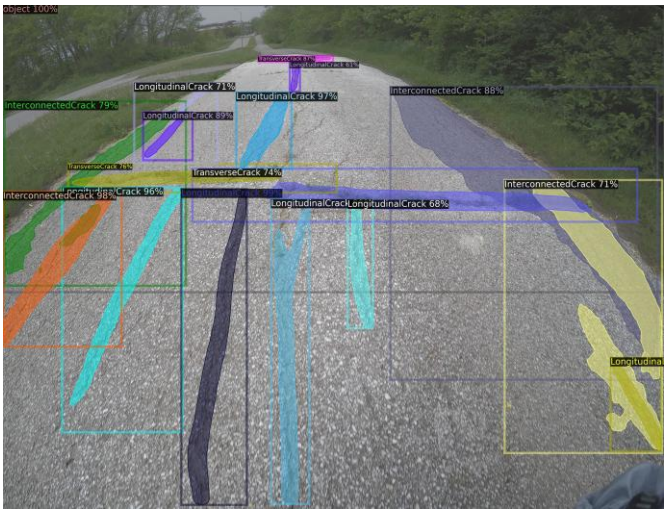
Model performance on AC surface:

- Good detection capacity on critical distress type (i.e., interconnected cracks)



Model performance on AC surface:

- Performance on heavily cracked areas



Model performance on AC surface:

- Performance on trails in good condition

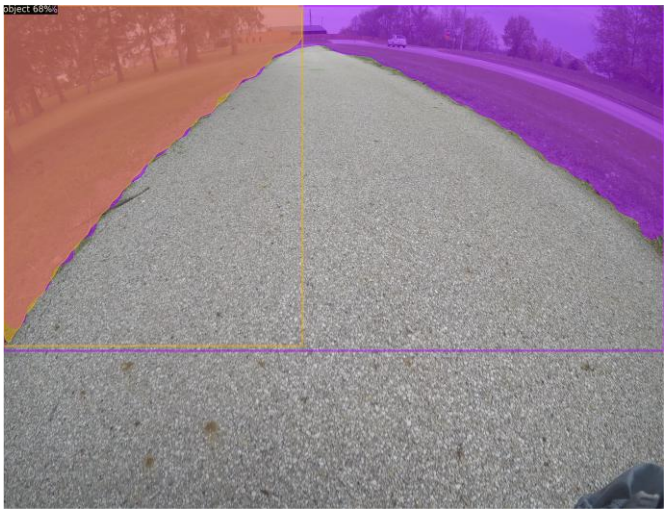
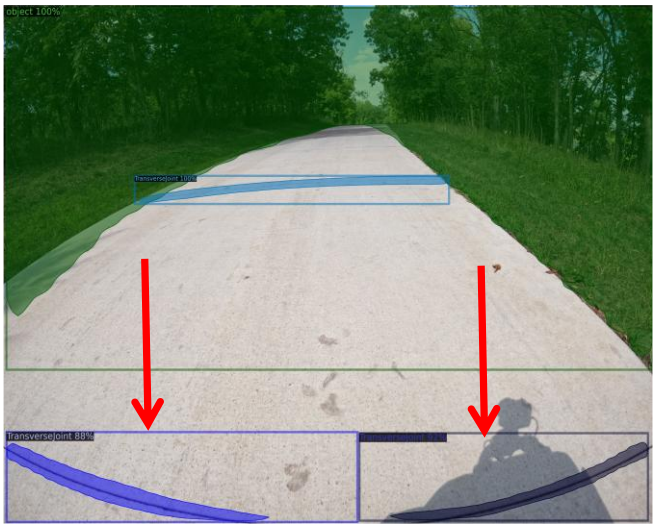


Figure 18. Model prediction evaluation

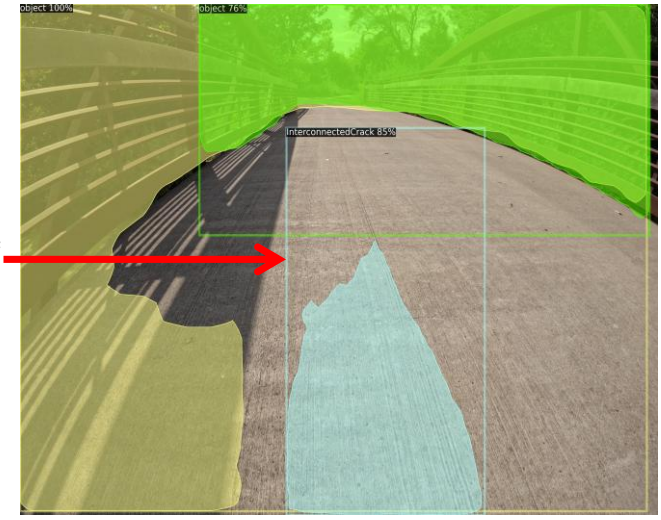
Model Limitations

The Mask R-CNN model for trail distress detection exhibits few limitations, as illustrated by Figure 19. For instance, the model incorrectly identifies crack-like textures on PCC surfaces as interconnected cracks. This misclassification indicates the model's difficulty in distinguishing between actual cracks and similar surface textures, potentially leading to false positives. Also, the model fails to detect transverse joints that are located farther away on the PCC surface. This limitation suggests a potential issue with the model's sensitivity or its ability to accurately identify features at varying distances. Additionally, image distortion has resulted in a single joint being erroneously detected as two separate joints. This distortion and subsequent misclassification highlight the model's susceptibility to variations in image quality and angle, which can influence the accuracy of the detected instances. Moreover, there are some overlap of prediction instances observed in areas with heavy cracking. This overlap indicates the model's challenge in differentiating and correctly segmenting densely cracked regions, leading to multiple predictions for the same distress area. Such redundancy can complicate the analysis and interpretation of the distress extent. These identified limitations highlight the need for further refinement of the Mask R-CNN model to enhance its accuracy and reliability in detecting trail distress. Potential improvements could include enhancing the model's training dataset with more diverse and high-quality images, implementing advanced image processing techniques to mitigate distortion effects, and refining the model's algorithm to better differentiate between similar surface features and accurately segment densely cracked areas.

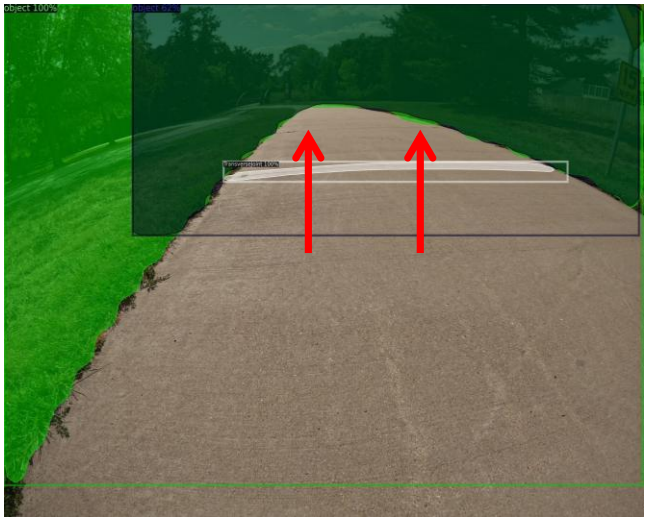
One joint detected as two due to image distortion



Crack-like surface texture on PCC surface predicted as Interconnected Crack



Transverse Joints far-away not detected on PCC surface



Overlap of prediction instances on heavily cracked area

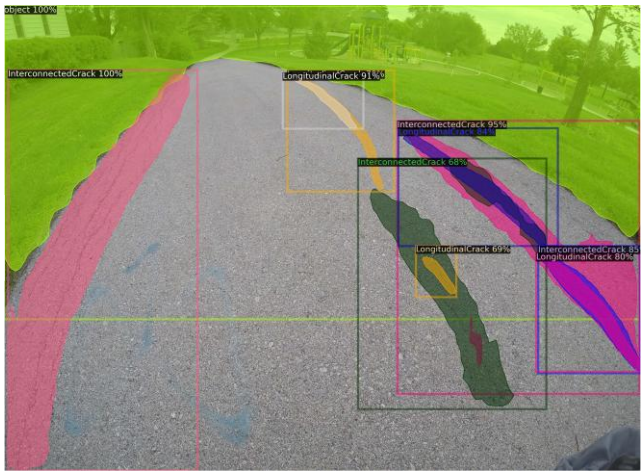


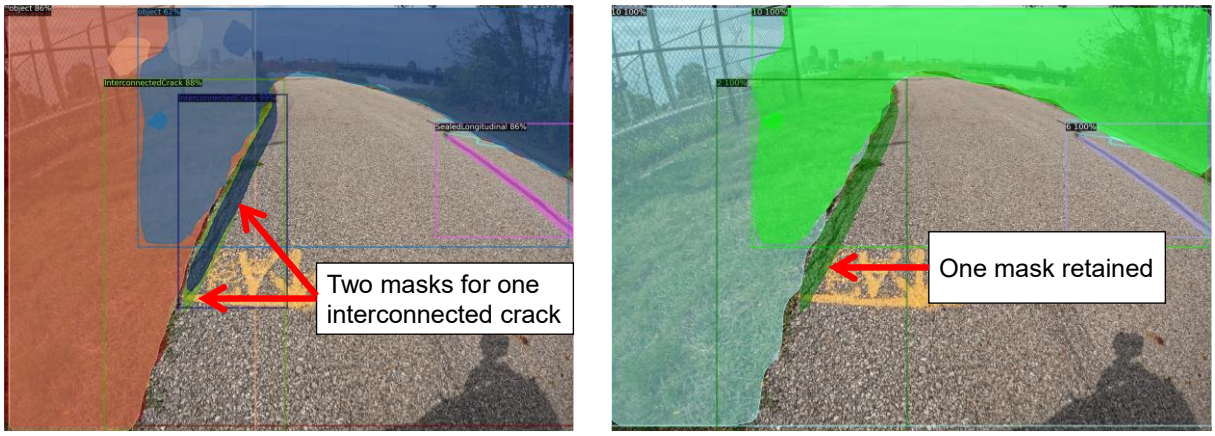
Figure 19. Instances showing model limitations

Filtering Prediction Redundancy

As discussed above, the model's prediction instances overlapped in heavily cracked areas that may lead to misinterpretation of the distress extent within an image. Therefore, in this study we implemented a filtering function prioritizing certain categories of cracks and systematically removes redundant or less significant masks based on their area and category-specific priorities. These overlapping instances were observed mostly in cracks in the longitudinal direction with different classes such as longitudinal cracks, interconnected cracks, and sealed longitudinal cracks. Initially, the priority levels are defined for each these categories, where interconnected cracks have the highest priority, followed by longitudinal cracks, and sealed longitudinal cracks with the lowest priority.

The primary filtering function operates in two main passes. In the first pass, it iterates over each item in the dataset, comparing it with every other item to calculate the IoU between their masks. If two masks belong to the same category and have an IoU greater than 0.6 or one is a subset of the other, the smaller mask is removed. If the masks belong to different categories, the one with a lower priority is removed based on the overlap or subset relationship. The second pass of filtering focuses on removing subsets within the same category. For each item, it checks if its mask is a subset of any other mask within the same category, ensuring that only the most relevant and significant masks are retained. This two-step process effectively refines the dataset, prioritizing masks that provide the most critical and distinct information for further analysis.

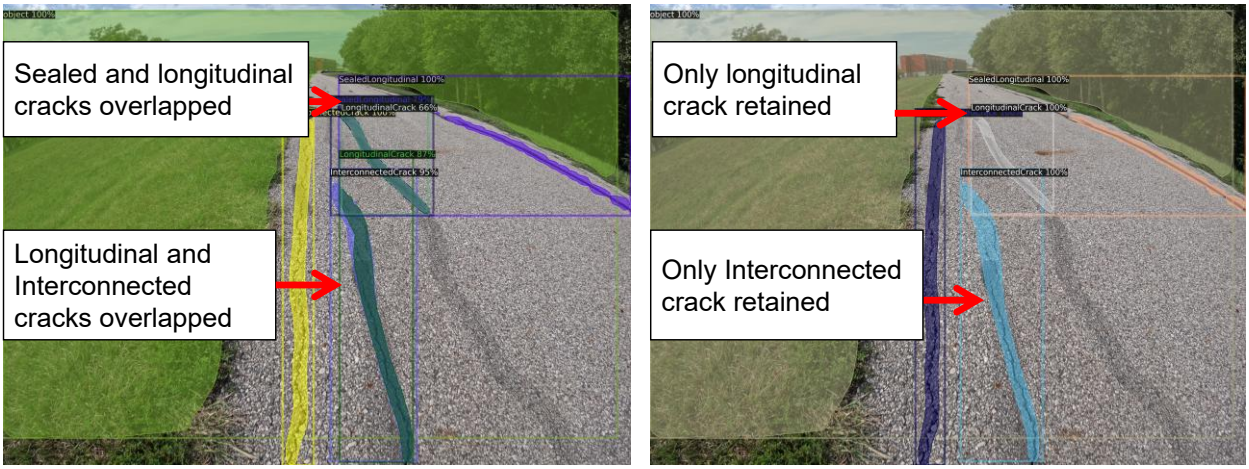
For example, as illustrated in Figure 20, the comparison of the model's output before and after applying the filtering algorithm demonstrates its efficacy. Initially, the model identified two interconnected areas of distress, which, upon closer inspection, were adjacent and effectively impacted the same location. This redundancy indicates that a single interconnected crack would sufficiently represent the distress extent in that area. After applying the filtering algorithm, the extraneous interconnected crack was removed, resulting in a more accurate representation of the distressed trail.



a) Before mask filtering b) After mask filtering

Figure 20. Comparison of model output before and after filtering algorithm application

Another example is illustrated in Figure 21, comparing the model output before and after the implementation of the filtering algorithm. The left image shows the initial model output, where sealed longitudinal cracks and longitudinal cracks, as well as longitudinal crack and interconnected crack, overlap. After applying the filtering algorithm, as shown in the right image, only the most representative cracks are retained. Specifically, only one longitudinal crack is retained from the overlapping sealed longitudinal and longitudinal cracks, and only the interconnected crack is retained from the overlapping interconnected and longitudinal cracks.



a) Before mask filtering b) After mask filtering

Figure 21. Comparison of model output before and after filtering algorithm application

SURFACE DISTRESS QUANTIFICATION

The predicted masks from the computer vision models were processed and analyzed to quantify the actual extent of surface distresses on ground. Capturing images with GoPro cameras, which often result in distorted, wide-angle, and oblique view images, posed a significant challenge in accurately measuring the length or area of the surface distress. To overcome this, we employed a scaling factor derived from extensive experimentation with GoPro camera. This process involved capturing images of objects with predetermined lengths, designed to simulate longitudinal and transverse cracks located at different parts of the images. After that, we were able to establish a reliable scale by comparing the predicted masks from the computer vision models with these known dimensions (i.e., the ground truth). This scaling factor is essential for converting the dimensions within the predictive masks into real-world measurements.

The development of the scale model involves several steps, which are detailed below:

- **Image Capture**: Images are captured using a tilted camera mounted on a bicycle running along a trail segment.
- **Tape Representation**: Tapes representing cracks (both transverse and longitudinal) with known lengths are placed on the trail segment as shown in Figure 22. These tapes serve as reference objects for calibration.
- **Tape Detection**: The tapes are detected from the captured images using a computer vision model. This model identifies the bounding boxes around the tapes, allowing for precise measurement.
- **Pixel Measurement**: The length and width of the tape in pixels are measured from the detected bounding box. These pixel measurements are crucial for determining the scale.
- **Distance Measurement**: The distance from the bottom of the image to the center of the bounding box is measured. This distance helps in understanding the position of the detected object within the image.
- **Nonlinear Regression Model**: A nonlinear regression model is developed to represent the relationship between the scale (true length divided by pixel length) and the distance from the bottom of the image. This model accounts for the nonlinear distortion caused by the camera tilt.
- **True Length Estimation**: Using the scale value obtained from the regression model, the true length of detected distresses can be estimated. This is done by multiplying the pixel length measured from the image by the scale value.

In order to calculate the distance (in pixels) from the bottom of the image to the center of the bounding box, the following equation is used and the process is illustrated in Figure 22.

$$Distance = \frac{X_1 + X_2}{2} \tag{14}$$

where X_1 and X_2 are the distance (in pixels) from the bottom of the image to the bottom and top of the bounding box, respectively.

The relationship between the scale of transverse cracking and T-joint with the distance from the bottom of the image to the center of the bounding box is represented by the following equation:

$$\text{Scale} = \text{Exp}(4.9655 \times 10^{-12}(\text{Distance})^{4.1659} - 4.6286) \quad (15)$$

This equation indicates how the scale varies nonlinearly with the distance, compensating for the camera tilt effect. The exponential function effectively models the complex distortion introduced by the tilted camera setup as shown in Figure 22. Using this scale value, the true length of the distress can be estimated by multiplying the scale by the pixel length measured from the image:

$$\text{Length (ft)} = \text{Scale} \times \text{Length (px)} \quad (16)$$



Figure 22. Tapes with known lengths placed on the trail segment for calibration

Using the same molding technique, the relationship between the scale of longitudinal crack with the distance from the bottom of the image to the center of the bounding box as shown in Figure 23 is represented by the following equation:

$$\text{Scale} = \text{Exp}(1.8262 \times 10^{-13}(\text{Distance})^{4.7679} - 4.4902) \quad (17)$$

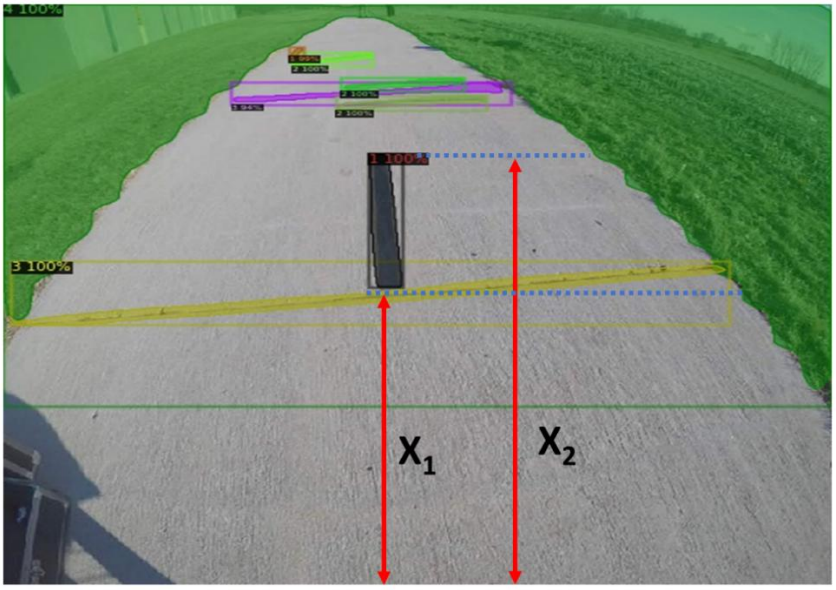


Figure 23. Illustration of the process to calculate the distance from the bottom of the image to the center of the bounding box

Using this scale value, the true length of the distress can be estimated by multiplying the scale by the pixel length measured from the image:

$$\text{Length (ft)} = \text{Scale} \times \text{Length (px)} \tag{18}$$

In addition to estimating the true length of detected distresses, accurately estimating the area of patches required for maintenance on trails is crucial. The estimation of patching area depends on the longitudinal and transverse crack models mentioned in equation (15) and equation (17). Using the scales obtained from the above models, the area of the patch can be computed. The area is calculated by multiplying the scaled length and width of the distress in pixels:

$$\text{Area}(\text{ft}^2) = (\text{Scale1} \times \text{Length (px)}) \times (\text{Scale2} \times \text{Width(px)}) \tag{19}$$

where Scale1 is represented in equation (17) and Scale2 is represented in equation (16).

This model allows for the estimation of the area required for patching, ensuring that maintenance efforts are both effective and efficient. By combining the transverse and longitudinal scale models (as shown in Figures 24 and 25), the patching model accounts for the varying scale effects within the image due to camera tilt, resulting in accurate area measurements for trail maintenance.

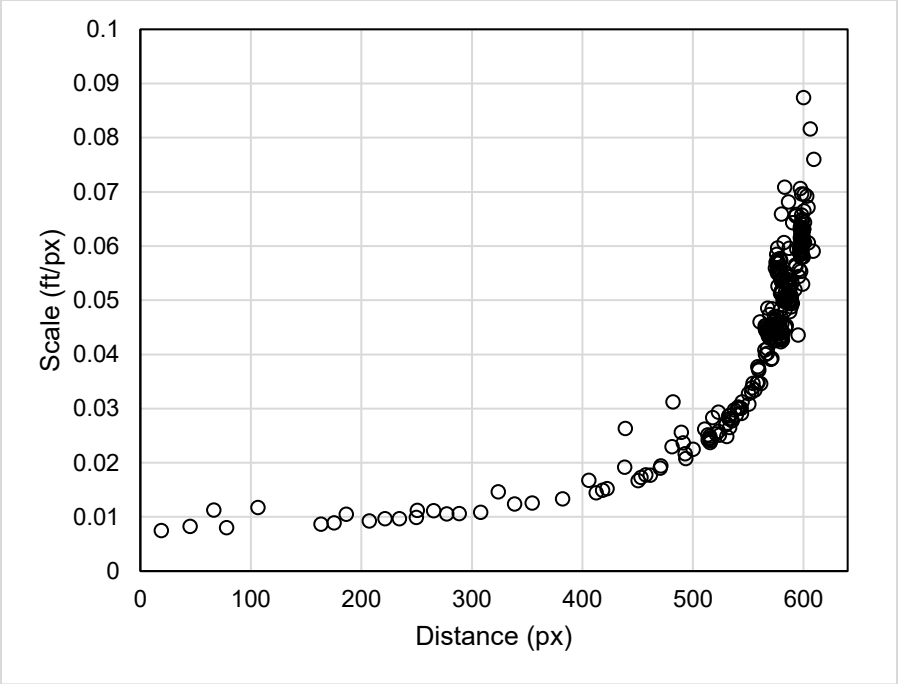


Figure 24. Scale for transverse cracking and T-joint

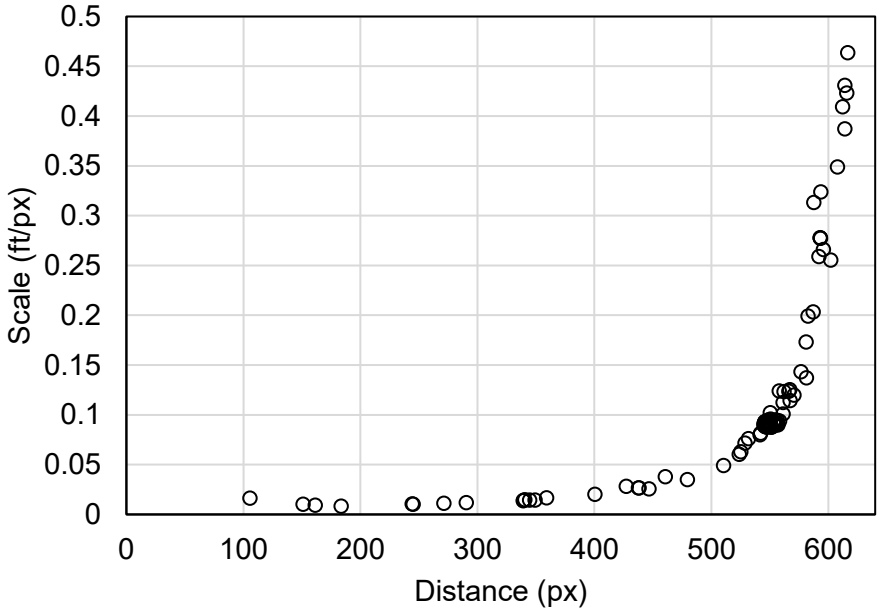


Figure 25. Scale for longitudinal cracking

Scale Model Validation

The scale models were validated by comparing the estimated lengths and areas to known reference lengths. This involved using tapes with precise, pre-measured lengths and widths

placed on the trail segment. Images of these tapes were captured using the tilted camera setup on the bicycle, replicating the conditions under which the scale models were developed. The transverse and longitudinal scale models were applied to these images to estimate the true lengths and areas. The estimated measurements were then compared to the known measurements. As shown in Figure 26, the comparison demonstrated that the scale models provided reasonable accuracy.

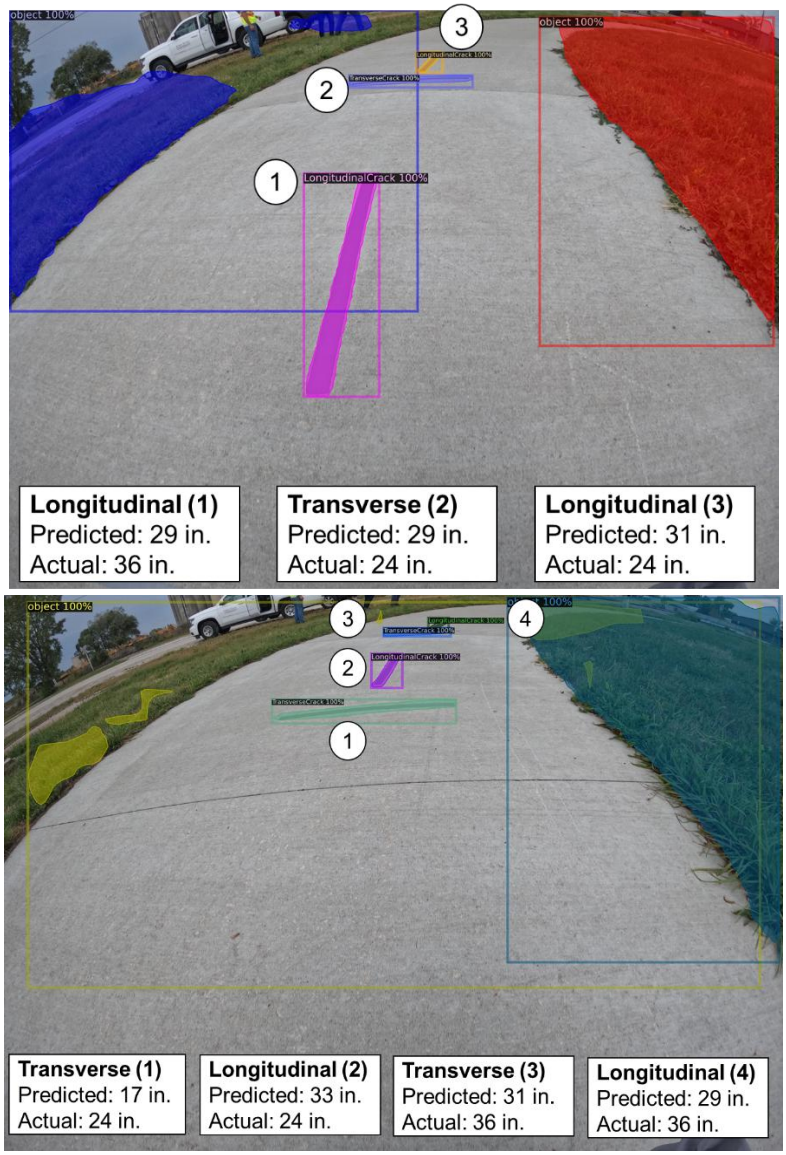


Figure 26. Results from validation experiments for the scale model

Specifically, the differences between the estimated and actual measurements were within acceptable limits, as detailed below:

- **Longitudinal Measurements**: For instance, the predicted length of 29 in. for a longitudinal crack was compared to the actual length of 36 in., while another predicted length of 31 in. matched the actual length of 24 in.
- **Transverse Measurements**: Similarly, the predicted length of 17 in. for a transverse crack was compared to the actual length of 24 in., while another predicted length of 31 in. closely matched the actual length of 36 in.

This validation supports the effectiveness of the scale models accounting for camera tilt, ensuring reliable measurements for the extent of trail distresses from GoPro imagery. The scale for the longitudinal and transverse dimensions can used to calculate the extent of area-based distresses such as interconnected cracking and patching.

NETWORK-LEVEL DEPLOYMENT

The final phase of the trail management program involved the network-level deployment of the developed algorithms for roughness indices (i.e., BRI) and distress data quantified from georeferenced imagery. This deployment involved applying the established frameworks to historical data captured by the Iowa Data Bike and integrating the condition data into a GIS-based environment.

The vertical motion data collected by the smartphone accelerometer mounted on the Iowa Data Bike was utilized to estimate the BRI for the trail network. Accelerometer data from 2024 covered approximately 175 mi at a sampling frequency of 100 Hz. This data was processed to calculate the BRI (in./mi) while preserving its geospatial attributes. Based on the BRI distribution across the entire trail network, roughness levels were categorized into three classes: good, fair, and poor, as illustrated in Figure 27.

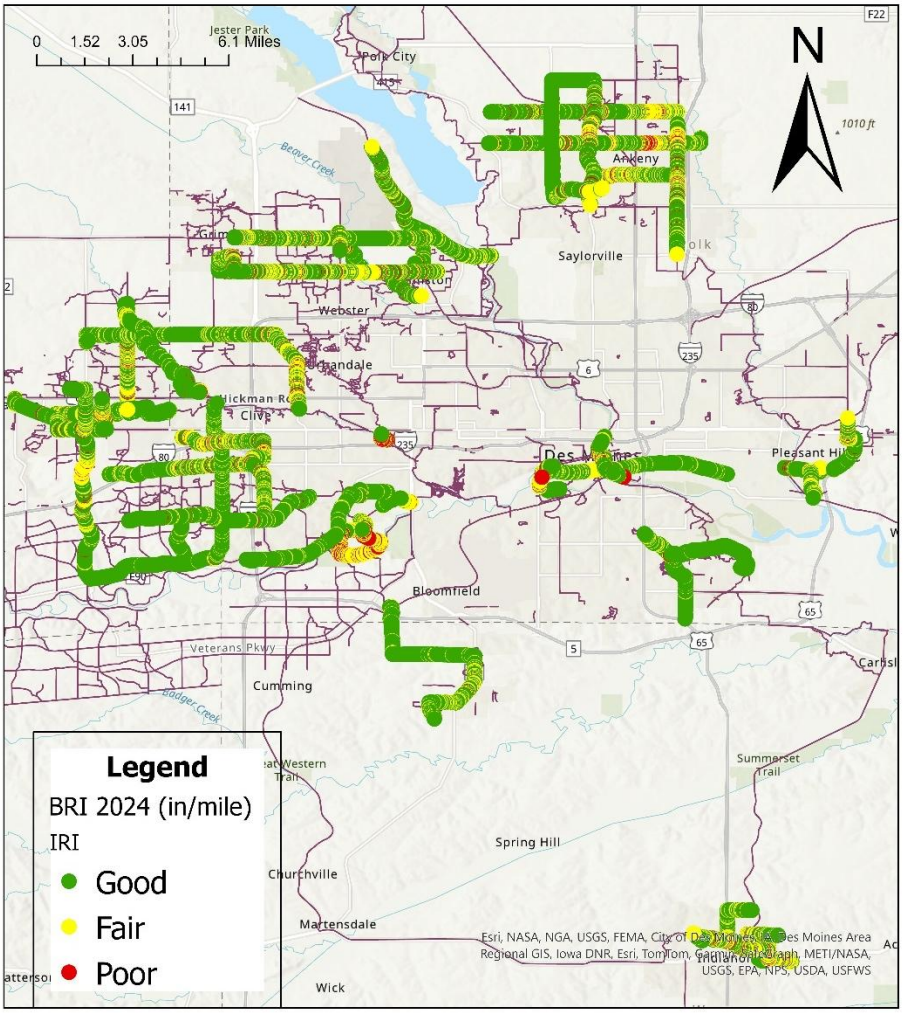


Figure 27. Trail condition based on BRI

Integrating Automated Distress Evaluation Framework with Historical Data

Since 2017, the Des Moines Area MPO's Iowa Data Bike has been systematically capturing network-level historical data on trail conditions, as shown in Table 3. In this study, we developed an algorithm to process network-level images for instance segmentation using the Mask R-CNN model. The goal is to automate the detection and quantification of trail surface distresses by integrating the results into a GIS-based environment for enhanced trail management. The tool automates the identification and classification of trail surface distresses by traversing directories containing images and identifying relevant files for analysis, which ensures that the algorithm systematically handles extensive datasets. Each image is read, and predictions are generated using the trained Mask R-CNN model. Relevant metadata, such as image coordinates and date-time information, is extracted. These predictions identify and classify various types of trail surface distress.

Table 3. Number of images collected and filtered for the trail network

Year	Number of Images before Filtering	Number of Images after Filtering
2017	882	786
2018	67031	25333
2019	35044	22112
2020	35670	17703
2021	52694	31493
2022	6152	3214

The next step involves organizing and storing the prediction results and metadata in a structured format. Predictions and metadata are compiled into dictionaries and saved as pickle files. This structured storage facilitates easy retrieval and integration into other systems. Organizing prediction results and metadata systematically ensures data integrity and traceability through the use of unique identifiers, making the data easy to retrieve and analyze. The pickle files can be imported for further processing steps, such as filtering prediction redundancies and applying a scaling model. The results, along with relevant metadata from the images and distress data, are then saved in a CSV file. Finally, the processed data is integrated into a GIS-based environment as point features, as shown in Figure 28, where each point represents an image, and the distress data obtained from that image are stored as attributes of the points. It was observed that some trail segments contained redundant or duplicate images, which were filtered using a dedicated algorithm to ensure a consistent image frequency for trail segments across different years.

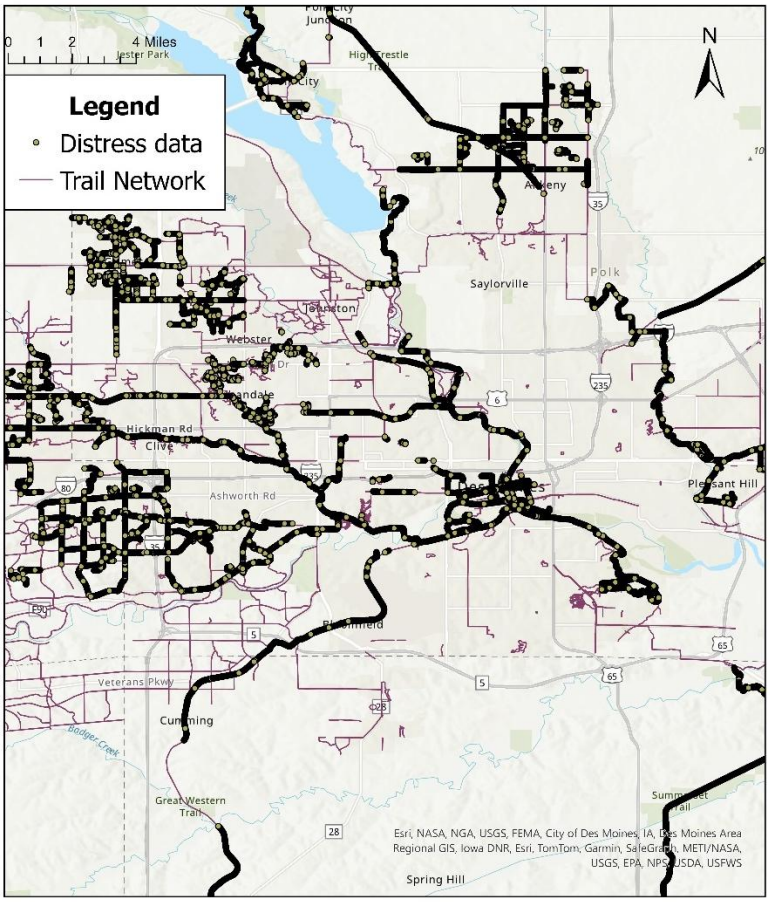


Figure 28. Distress data quantified from images for the trail network

Refining Image Frequency

To ensure accuracy and efficiency in analyzing trail condition data, a process was developed using ArcGIS Pro to filter duplicate data points collected on the same trail segment at the same time. The methodology utilized for this purpose is illustrated in Figure 29. The process begins with importing two key datasets into the GIS environment: the trail condition data as a points shapefile and the trail history shapefile delineating the spatial extents of each trail segment within the network. The trail history shapefile segments are pre-divided into shorter sections, typically 24 ft in length, each assigned a unique identifier. This segmentation allows for precise spatial referencing and analysis at the segment level. Subsequently, the condition data points are spatially joined to the segmented trail history shapefile. This spatial join operation assigns each data point to its corresponding trail segment based on spatial proximity.

Following the spatial join, redundant data points are identified and filtered out using attribute queries and spatial selection techniques within ArcGIS Pro. Specifically, duplicate data points collected on the same segment of the trail at identical timestamps are identified, and only one representative data point per segment is retained for further analysis. This ensures that the dataset remains concise and accurate, reflecting a single data point per trail segment during subsequent

analyses and reporting. All these filtering steps were performed in ArcGIS Pro, where an automated tool was developed to facilitate the process, as illustrated in Figure 29.

Upon further evaluation, it was observed that this de-duplication approach—while effective in reducing data redundancy—introduced unintended data gaps in the trail network. To address this, the methodology was revised to retain all collected points but aggregate them within each 24 ft trail segment by computing the average value for each condition metric. This revised approach offered two advantages:

- **Preserved full data density**: By not discarding any points, full spatial granularity of observations was maintained.
- **Enabled coverage estimation**: The revised method enabled calculation of coverage metrics, indicating the proportion of each segment with valid condition data.

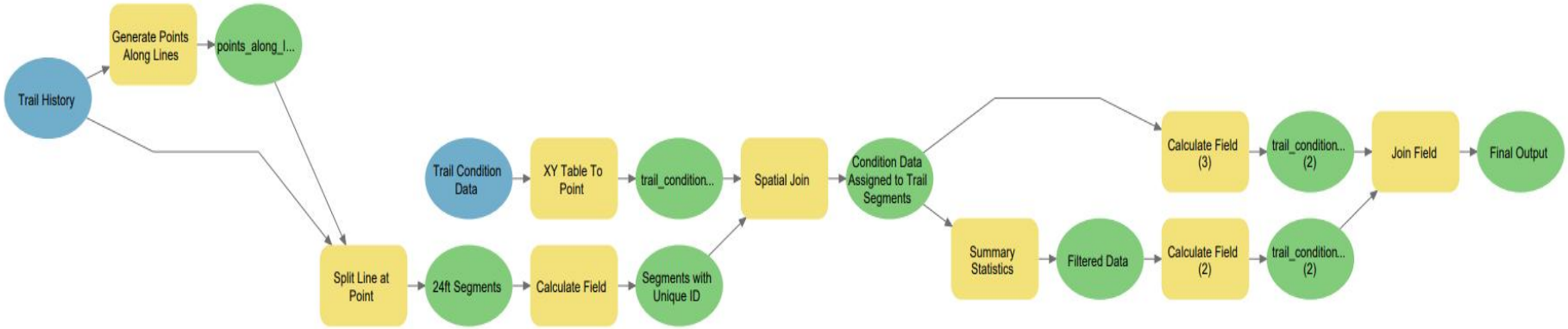


Figure 29. ArcGIS-based automation tool for refining image frequency at the network level

Data Quality Assessment and Outlier Detection

To ensure the reliability and accuracy of distress measurements for network-level analysis, an automated outlier detection methodology was implemented using the interquartile range (IQR) method. This approach systematically identifies and flags trail segments containing extreme distress values that may result from measurement errors, image quality issues, or anomalous detection events during automated processing.

The outlier detection algorithm analyzes nine distress measurement categories: interconnected cracking, longitudinal cracking, object detection, patching, pothole, sealed longitudinal cracking, spalling, T-joints, and transverse cracks. Using an IQR multiplier of 2.0, the method identifies outliers within each distress category by calculating the first quartile (Q1), third quartile (Q3), and IQR, then flagging values that fall outside the bounds of Q1 - 2.0 × IQR and Q3 + 2.0 × IQR. This conservative approach ensures that only the most extreme measurements are flagged while preserving legitimate high-distress readings.

The algorithm processes each distress category independently, recognizing that different distress types exhibit varying measurement ranges and distribution characteristics. This category-specific approach ensures that outlier detection thresholds are appropriately calibrated for each distress type's expected measurement range.

Application of this methodology to the 2024 network-level dataset containing 55,905 distress measurements revealed varying levels of outliers across different distress types. The analysis removed measurements from all categories, with transverse cracks showing the highest number of removed measurements (754 instances), followed by longitudinal cracking (496 instances), T-joints (293 instances), and sealed longitudinal joints (275 instances). The remaining categories showed lower removal counts: interconnected cracking (228), patching (56), spalling (3), and potholes (3). After removing 1,204 total measurements, the cleaned dataset retained 54,701 rows, representing an overall 97.8% data retention rate.

Retention rates varied across distress types, ranging from 91.2% for pothole measurements to 99.3% for spalling measurements. Most categories achieved retention rates above 93%, indicating that the outlier detection process effectively identified anomalous measurements while preserving the majority of valid data for each distress type.

Figure 30 illustrates the distribution of distress measurements before and after outlier removal, demonstrating the effectiveness of the filtering process in eliminating extreme values while preserving the overall data distribution characteristics. This data quality enhancement step ensures that subsequent network-level analyses and performance assessments are based on reliable measurements, thereby improving the accuracy of maintenance planning and decision-making processes.

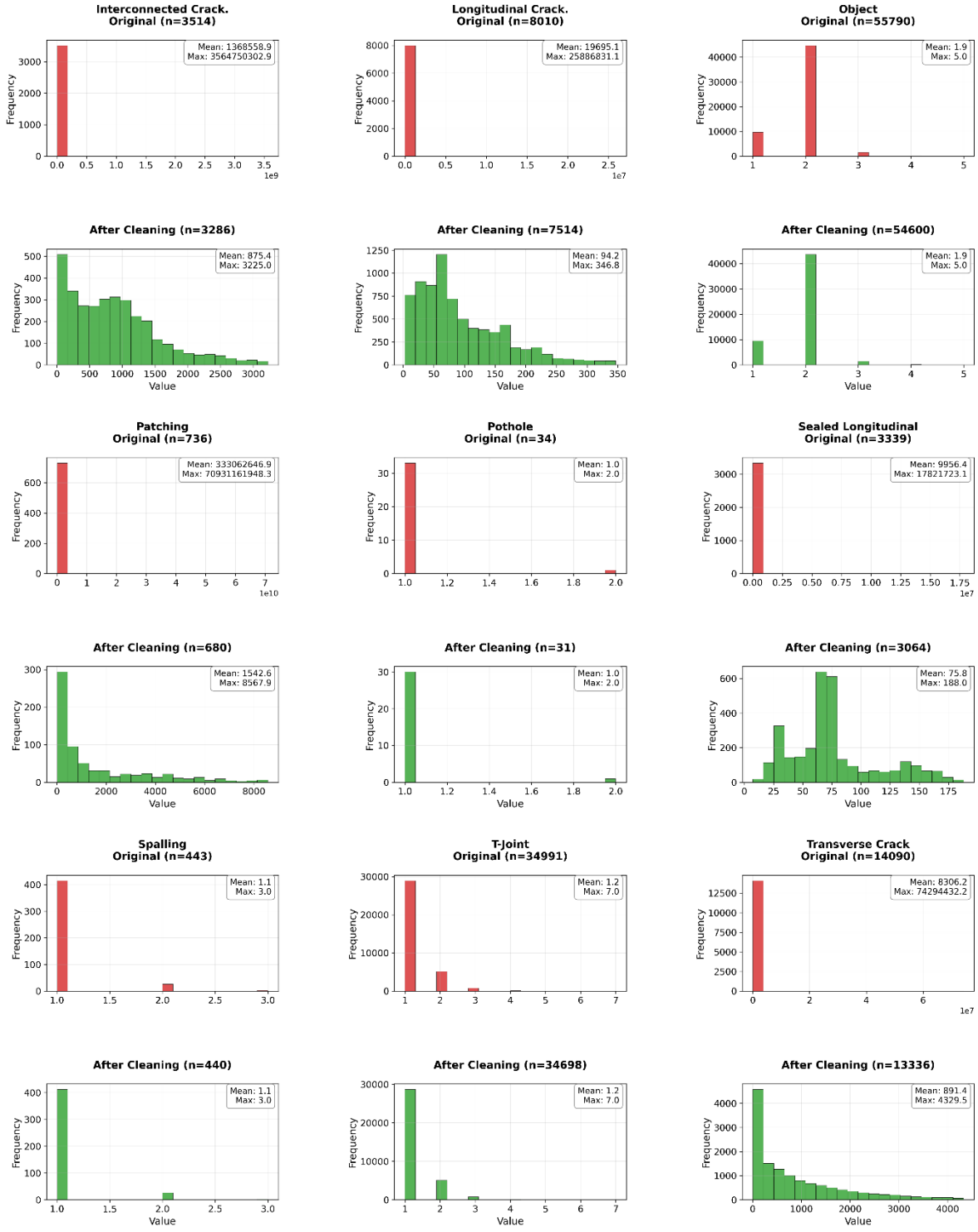


Figure 30. Distribution of distress measurements before and after IQR-based outlier removal, showing 97.8% data retention with 1,204 outliers removed from the dataset

Time-Series Assessment of Distress-Level Trail Condition

This section presents an evaluation of automated distress data obtained from GoPro imagery to assess the performance of the detection method developed for this project. The assessment highlights data quality issues and identifies opportunities for improving both data quality and automated detection processes. Historical data points (i.e., images) were spatially matched to the nearest trail segments using a unique identifier known as ParkID. The inventory consisted of 4,860 trail segments, each varying in length and surface characteristics.

Figure 31 illustrates a representative example of this evaluation. The map on the left highlights the spatial location of a selected trail segment (ParkID 2709), while the panel on the right displays the time-series summary of detected distress features for the years 2018 and 2019. The stacked bar chart captures the distribution of various distress types over time, including interconnected cracking, longitudinal cracking, patching, sealed longitudinal cracking, spalling, and transverse cracking.

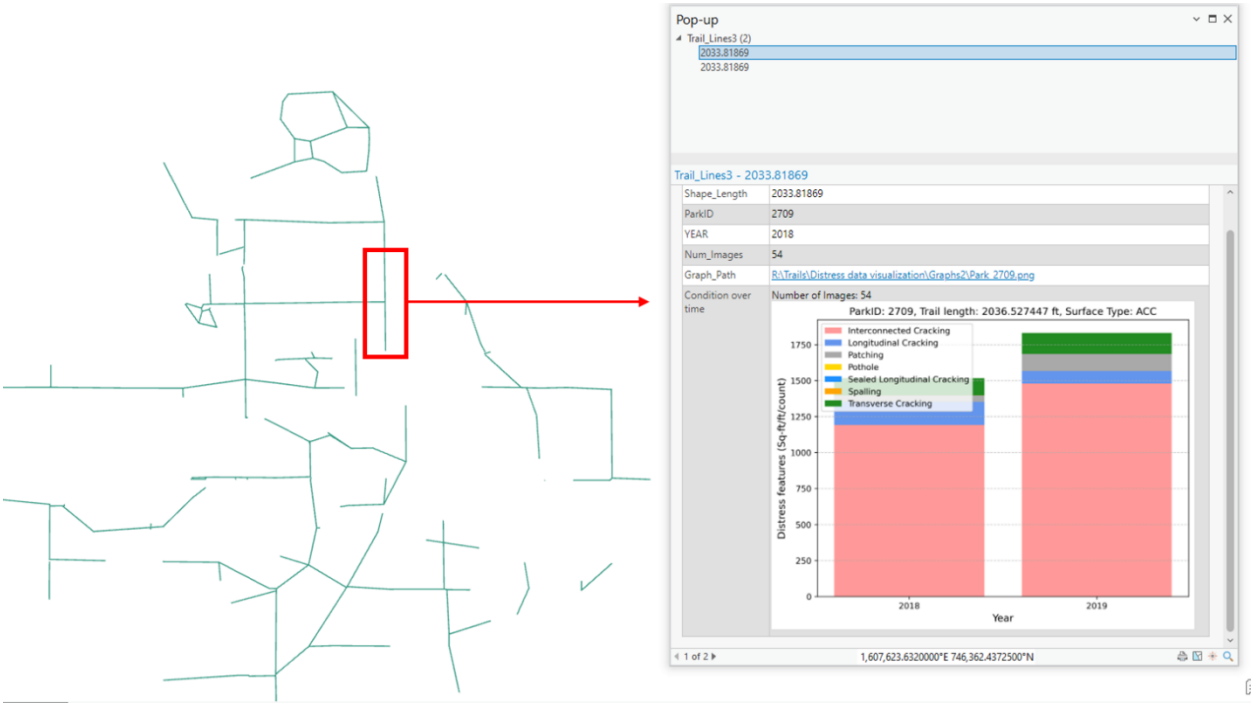


Figure 31. Example of time-series trail condition assessment for ParkID 2709

However, data availability posed certain limitations, as historical images were available for only 2,045 segments. As shown in Table 4, the number of trail segments with long-term data was relatively limited—only 481 segments had data spanning at least two years, while just 14 had data extending over five years. Additionally, the dataset exhibited inconsistencies in image volume across segments; for instance, 934 segments had fewer than 10 images, and only 751 segments had at least 20 images. These gaps in data coverage and inconsistency in image counts over time underscore challenges in conducting robust longitudinal distress assessments.

Table 4. Trail segments with available historical data

Total number of ParkIDs with available data	2045
Number of ParkIDs with data over 2 years	481
Number of ParkIDs with data over 3 years	166
Number of ParkIDs with data over 4 years	71
Number of ParkIDs with data over 5 years	14
Number of ParkIDs with less than 10 images	934
Number of ParkIDs with less than 15 images	1155
Number of ParkIDs with less than 20 images	1294

For instance, examining the distress progression for segments with four years of historical data, ParkIDs 1045 and 1728, as shown in Figures 32 and 33, both exhibited consistent growth in surface distresses over time. These trends reflect the natural aging and deterioration of trail infrastructure in the absence of significant maintenance interventions. However, a noticeable decline in distress quantities observed in the final year for ParkID 1728 may not indicate true surface improvement but rather result from inconsistencies in data collection.

Park ID:1045	
Year	# Images
2019	26
2020	38
2021	49
2022	46

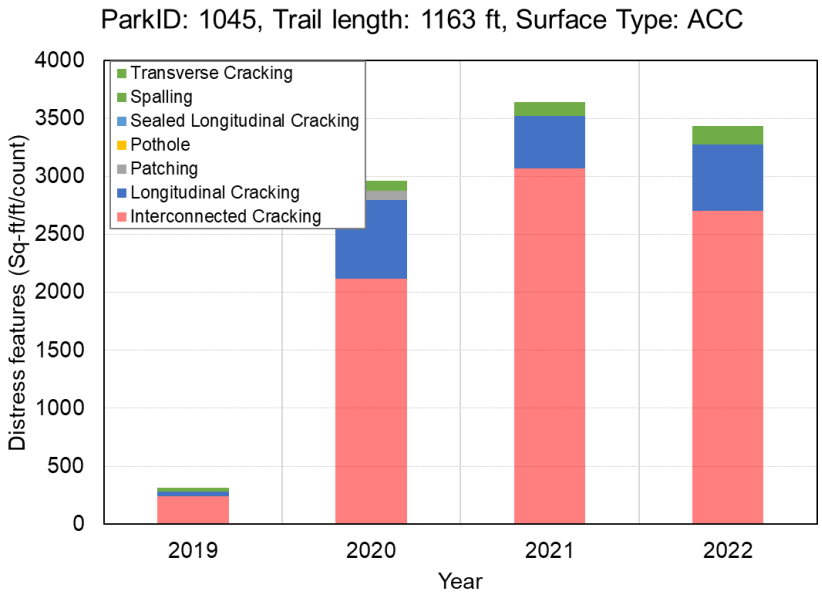


Figure 32. Distress progression over four years: ParkID 1045

Park ID:1728	
Year	# Images
2019	23
2020	34
2021	48
2022	45

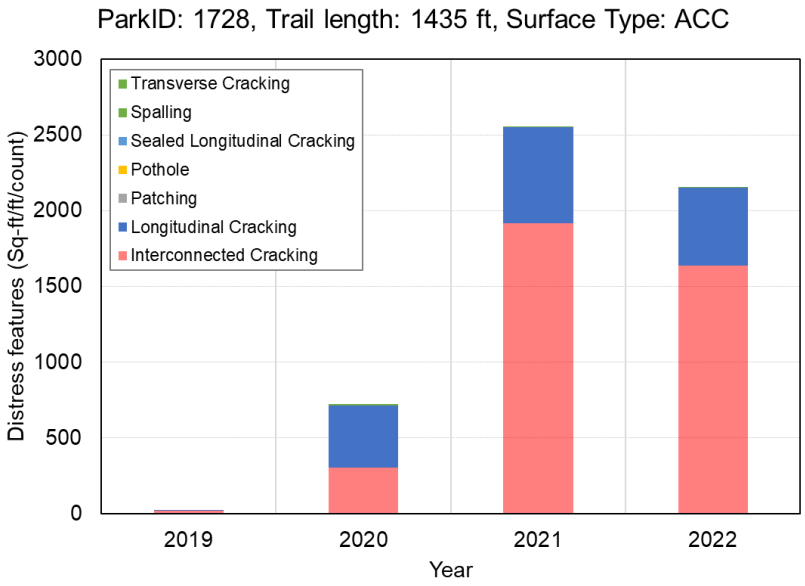


Figure 33. Distress progression over four years: ParkID 1728

As illustrated in Figure 34, the spatial distribution of images along ParkID 1728 in 2022 was uneven, with clear gaps in coverage across portions of the trail segment. Such incomplete image representation can limit the automated model's ability to detect and quantify distresses, particularly when image-based measurements are sensitive to feature visibility and position. This reinforces the importance of maintaining consistent and comprehensive image collection protocols to support reliable trend analysis over time.

Park ID:1728	
Year	# Images
2019	23
2020	34
2021	48
2022	45



Figure 34. Image distribution along ParkID 1728 for 2020–2022

In summary, the assessment showed overall distress progression across trail segments, though inconsistencies in image coverage affected detection reliability in some cases. These findings emphasize the need for consistent data collection and improved quality control to support accurate long-term monitoring.

DATA COLLECTION GUIDELINES

To establish robust guidelines for future data collection using the Iowa Data Bike, an experimental program was conducted on a selected test site. The site, a concrete-surfaced trail, featured simulated transverse joints and transverse cracks using tape markers. The experiment aimed to determine the optimal image capturing interval and camera angle for accurately capturing trail distresses.

Experimental Setup and Analysis

Data collection was performed using the Iowa Data Bike, which captured images at two different intervals (0.5 seconds and 2 seconds) and two different camera angles (30° and 45°). Figure 35 shows the geo-referenced images captured under different data collection configurations. The specific configurations and their results are outlined in Table 5.

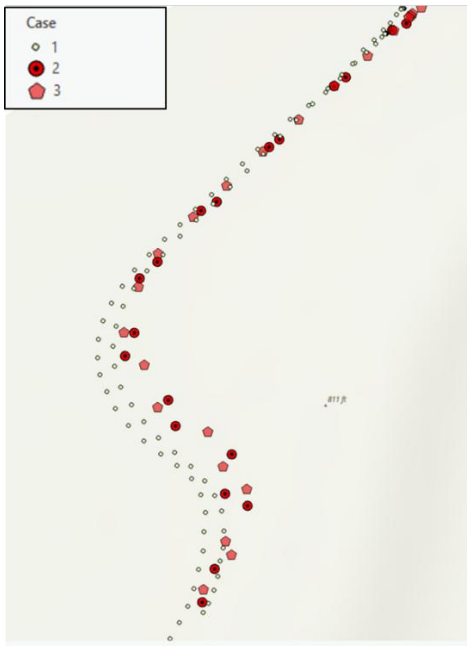


Figure 35. Geo-referenced images from the experimental program plotted in GIS environment

Table 5. Experimental data collection configurations and results

Case No.	Photo Interval (Seconds)	Angle (°)	Number of Photos	T-Joint (Count)	Transverse Crack (Count)
1	0.5	45	42	20	11
2	2	30	10	6	3
3	2	45	10	6	4
Ground-truth				11	6

This table summarizes the experimental configurations and results for data collection on the testing site. It details the photo intervals, camera angles, number of photos captured, and the counts of detected transverse joints and transverse cracks for each case, compared to the ground-truth data. The objective was to determine the data collection settings that most accurately reflect the ground-truth counts of transverse joints and transverse cracks. The results indicated that a photo interval of 2 seconds with a 45° angle (Case 3) captured the closest number of distresses, with 6 T-joints and 4 transverse cracks, closely aligning with the ground-truth counts of 11 T-joints and 6 transverse cracks. This configuration ensures the most accurate capture of trail distresses, closely matching the ground-truth data.

Established Guidelines

Based on the analysis and findings of the experimental study, following data collection was established for bicycle-based trail data collection for surface smoothness and distress assessment.

A. **Riding Guidelines**

a. Ride Position
- Ride in the middle of the trail to ensure consistent data collection.

b. Direction of Travel
- Collect data in one direction only to maintain uniformity.

c. Shadow Management
- Avoid bicycle shadows in the images to prevent information loss.

d. Speed Consistency
- Maintain a consistent and reduced speed to ensure images are not motion-blurred.

B. **GPS Setup**

a. Initialization
- Turn on the GoPro camera at least 5 minutes before starting data collection to ensure the GPS is enabled and accurate.

C. **Bike Settings**

a. Tire Pressure
- Maintain consistent tire pressure throughout the data collection process to ensure reliable results.

D. **Camera Settings**

a. Angle Consistency
- Set the camera at a consistent angle of 45° to the trail surface.

b. Time-Lapse Configuration
- Use a time-lapse setting of 1 second for capturing images.

c. Camera Configuration
- Keep camera settings consistent for the duration of data collection.
  - Field of View: Wide Angle
  - Orientation: Oblique

DTIMS IMPLEMENTATION METHODOLOGY FOR TRAIL MANAGEMENT

The integration of the Deighton Total Infrastructure Management System (dTIMS) represents a critical advancement in applying systematic asset management principles to trail networks. While dTIMS has traditionally been employed for roadway and pavement management, its flexible framework provides an ideal platform for managing recreational trail infrastructure with the same rigor and data-driven approach used for major transportation assets.

The implementation of dTIMS for trail management leverages all data collection and analysis methodologies developed in this study, including the BRI, automated distress detection using Mask R-CNN, and comprehensive condition assessment protocols. This integration transforms disparate condition data into a cohesive asset management framework that supports strategic decision-making, optimizes maintenance investments, and ensures the long-term sustainability of trail networks.

Data Integration and Asset Inventory

Trail segments were defined using available spatial and attribute data collected through the Iowa Data Bike, with each segment linked to unique identifiers and jurisdictional boundaries. The comprehensive inventory integrates multiple data sources developed throughout this study:

- **Spatial and geometric data**: GPS coordinates, latitude, longitude, and speed data collected at a 100 Hz sampling frequency, covering approximately 175 mi of trail network from the 2024 data collection.
- **Surface condition data**: Vertical motion data from smartphone accelerometers used to calculate the BRI, providing quantitative measures of trail surface quality AC and PCC segments.
- **Visual condition assessment**: Continuous geo-referenced imagery captured by GoPro cameras, processed through the automated Mask R-CNN detection system to identify and quantify trail surface distress.

Data from the Iowa Data Bike, supplemented with agency records and visual inspections, provided a comprehensive inventory of trail assets integrated into the dTIMS framework for systematic asset management.

Condition Assessment and Performance Metrics

Key trail condition metrics were established through the comprehensive data collection and analysis methodology developed in this study, including the following:

BRI: A quantitative measure calculated from smartphone accelerometer data collected via the Iowa Data Bike. The BRI classification system establishes five distinct condition categories, as presented in Table 6.

Table 6. BRI classification system for trail condition assessment

BRI Value (in./mi)	Category
≤ 265.18	Excellent
265.18–324.08	Good
324.08–382.97	Fair
382.97–441.87	Poor
> 441.87	Very Poor

Interconnected cracking density: Area of interconnected cracking per square foot of trail surface, calculated from Mask R-CNN detection results and converted to real-world measurements using validated scaling models.

Crack intensity: Length of linear cracks (longitudinal and transverse) per foot of trail, quantified through Mask R-CNN automated detection results and converted to real-world measurements using validated scaling models.

Performance Curve Development

Performance curves were developed within the dTIMS framework to model the expected deterioration of trail conditions over time. These predictive models form the analytical foundation for forecasting future maintenance needs and optimizing treatment timing across the trail network.

- The **BRI performance curve** models the decline in trail surface riding quality over time, accounting for factors such as age, environmental conditions, and treatment history. This curve provides the basis for predicting when trail segments will transition between condition categories and require intervention.
- The **interconnected cracking density curve** tracks the development and expansion of connected crack networks per unit area over time. This deterioration model enables the prediction of structural distress progression and supports timing decisions for preventive treatments.
- The **crack intensity curve** monitors the increase in linear surface cracking per unit length, modeling the rate at which new cracks develop and existing cracks extend. This curve supports maintenance planning by forecasting crack-related deterioration patterns.

The performance curves were calibrated using local data collected through the Iowa Data Bike and expert input from trail management practitioners. This calibration process ensures that the predictive models accurately reflect local conditions and deterioration patterns specific to Central Iowa's trail network. These validated curves serve as the predictive foundation for scenario modeling and long-term asset management planning within the dTIMS framework.

Treatment Definition and Costing

Three primary treatment strategies were established within the dTIMS framework, each linked to condition thresholds and performance curve forecasts developed through this study:

- **Preservation treatments** focus on preventative maintenance strategies such as seal/joint sealing and surface treatments designed to extend trail service life. These interventions address minor defects before they progress to more severe distress states.
- **Minor rehabilitation** encompasses localized repair strategies, including patching, thin overlays, and targeted repairs for moderate distresses identified through the automated detection system. These treatments restore functionality while addressing deterioration before more extensive intervention is required.
- **Replacement** involves full reconstruction of trail segments that have reached advanced stages of deterioration where surface and structural integrity have been compromised beyond the effectiveness of other treatment options.

Treatment costs were determined through direct engagement with local agencies and stakeholders involved in trail maintenance operations. This approach ensured that cost estimates reflect realistic local conditions and construction practices, enabling accurate scenario modeling and reliable budget forecasts for trail network management planning.

Decision Trees and Trigger Logic

Automated decision trees were established within the dTIMS framework to provide systematic treatment selection based on quantitative condition thresholds. These decision rules utilize the performance curves and condition metrics developed through this study to ensure consistent and objective treatment recommendations across the trail network.

The trigger logic incorporates both BRI values and specific distress measurements obtained through the automated detection system. This multi-criteria approach ensures that treatment decisions account for overall surface condition as well as specific distress characteristics that may influence treatment effectiveness and timing.

- **Preservation treatments** are triggered when trail conditions remain within acceptable performance ranges:
  - BRI ≤ 324.0 OR (interconnected cracking density < 50.0 OR crack intensity < 50.0)
- **Minor rehabilitation** is recommended for trails exhibiting moderate deterioration that falls between preservation and replacement thresholds:
  - BRI > 324.0 AND (interconnected cracking density < 75.0 OR crack intensity < 75.0)
- **Replacement** is indicated for severely deteriorated trail segments that have exceeded critical condition thresholds:
  - BRI > 400.0 OR (interconnected cracking density > 80.0 OR crack intensity > 80.0)

The systematic decision logic is illustrated in Figure 35, which provides a visual representation of the treatment selection process based on the established condition thresholds.

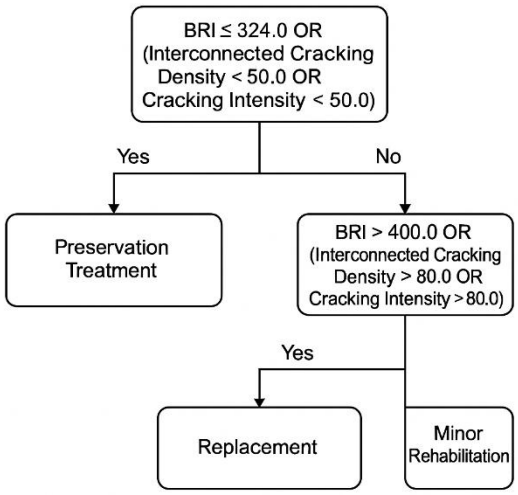


Figure 36. Trail treatment decision tree

The decision tree logic provides a systematic framework for treatment selection that eliminates subjective judgment while ensuring that maintenance interventions are applied at optimal timing to maximize cost-effectiveness and trail performance.

Scenario Modeling and Reporting

The dTIMS framework enables comprehensive scenario analysis to support strategic planning and investment decision-making for trail network management. Utilizing the performance curves, condition metrics, and treatment logic developed through this study, the system provides quantitative forecasting capabilities that evaluate different maintenance strategies and funding scenarios.

- **Condition forecasting** utilizes the calibrated performance curves to project future trail conditions under various treatment scenarios. These projections enable agencies to anticipate maintenance needs and evaluate the long-term impacts of different investment approaches on overall network condition.
- **Investment strategy analysis** evaluates the impacts of different funding levels on network performance, identifying optimal resource allocation strategies that maximize system-wide benefits. The analysis considers treatment costs established through local agency engagement and applies the automated decision tree logic to prioritize interventions across the trail network.
- **Reporting and visualization** capabilities provide actionable insights through multiple output formats designed to serve both technical and non-technical stakeholders. Key outputs include the following:
  - Condition projections based on performance curve modeling
  - Prioritized maintenance schedules generated through automated decision trees

- Budget requirements derived from validated treatment costs and network-wide condition analysis

GIS-enabled maps and graphical reports translate complex analytical results into accessible visualizations that support transparent decision-making and stakeholder communication. These reporting tools ensure that the technical rigor of the dTIMS analysis framework is effectively communicated to support informed trail management decisions.

Summary

The dTIMS implementation for trail management demonstrates a practical, replicable methodology that integrates the quantitative assessment techniques developed through this study. The framework combines smartphone-based BRI calculation, automated distress detection using Mask R-CNN, and systematic condition assessment protocols into a comprehensive asset management system.

This implementation approach transforms trail maintenance from reactive, subjective practices to proactive, data-driven management strategies. The integration of quantitative performance curves, locally validated treatment costs, and automated decision tree logic provides a systematic foundation for transparent resource allocation and strategic planning.

The framework supports improved user experience through optimized maintenance timing and ensures sustainable asset management across the trail network. By leveraging the comprehensive data collection and analysis methodologies established in this study, the dTIMS implementation provides trail management agencies with the analytical tools necessary for effective long-term infrastructure stewardship.

SUMMARY AND FINDINGS

This study not only developed innovative approaches for trail condition data collection and automated analysis but also integrated these methodologies into dTIMS. By embedding the BRI, deep learning-based surface distress detection, and systematic condition metrics within dTIMS, the project established a replicable framework for long-term, data-driven trail asset management. This integration transforms trail maintenance from reactive practices to proactive, strategic decision-making supported by quantitative performance models.

The trail management and assessment project detailed in this report employed advanced data collection and analysis methodologies to improve the maintenance and management of paved trails in Central Iowa. The primary objectives were to develop a standardized metric for assessing trail surface roughness and to create an automated framework for surface distress evaluation using deep learning techniques. The Des Moines Area MPO used its Iowa Data Bike—an electric-assist bicycle equipped with an iPhone and a GoPro camera—to collect detailed data on trail roughness and surface conditions. This data was processed to develop the BRI using accelerometer readings from the smartphone. Additionally, a computer vision-based automated framework for surface distress evaluation was developed using Mask R-CNN, a deep learning model for instance segmentation. Key findings, summarized below, include the effectiveness of the Iowa Data Bike in capturing comprehensive trail condition data, the accuracy of the BRI in reflecting surface roughness, and the success of the Mask R-CNN model in automating surface distress detection.

- **Data Collection Efficiency**: The Iowa Data Bike proved to be an efficient and comprehensive method for trail condition assessment. It facilitated rapid data collection over extensive trail networks, significantly reducing the need for traditional field inspections.

- **Roughness Metric Development**: The roughness of trail surfaces was effectively evaluated using two methods: double integration and whole-body vibration. These methods processed the vertical acceleration data collected from the smartphone to calculate the BRI and compared with roughness indices obtained from the reference profiler.

    - For AC trails, the whole-body vibration method outperformed the double integration method, with an R^2 value of 0.90 and an RMSE of 40.68.

    - For PCC trails, the double integration method was more accurate, with an R^2 value of 0.70 and an RMSE of 64.59.

- **Automated Distress Detection**: The Mask R-CNN model was trained to detect, classify and segment various types of pavement distress from the images captured by the GoPro camera. The automated detection system significantly reduced the need for manual inspection and improved the distress quantification for various distress classes.

- The developed model can reasonably classify and segment eight distress classes proposed for trail surfaces, such as longitudinal cracks, transverse cracks, interconnected cracks, sealed longitudinal cracks, potholes, patching, spalling, and transverse joints.

- Visual analysis confirmed that the model achieved high accuracy in identifying distresses in concrete surfaces compared to asphalt surfaces. The model performed satisfactorily for critical distress types such as interconnected cracking on asphalt surfaces. However, the model exhibited limitations such as misclassification of crack-like textures and difficulty in detecting distresses at varying distances.

- The filtering algorithm presented in this study successfully removed redundant predictions, enhancing the accuracy of the distress quantification process.

- **Quantification of Surface Distresses**: The predicted masks from the computer vision models were processed to quantify the actual extent of surface distresses. A scaling factor was derived to convert the dimensions within the predictive masks from oblique-angle imagery into real-world measurements, ensuring accurate length and area estimations for the distress classes.

- **Network-Level Deployment:**

  - The study deployed the automated distress detection model on the network-wide imagery and conducted a time-series condition assessment over five years. The key findings are as follows:

    - Most trail segments exhibited progressive distress over time, reflecting natural surface aging and deterioration. However, challenges such as automated scaling errors and model precision highlight the need for field calibration and additional training to improve the accuracy of the distress detection models.

    - Time-series assessments serve as valuable tools for identifying trail segments that have undergone maintenance actions and for detecting data quality issues related to image clarity, image count, and overall dataset consistency, which are essential for accurate distress analysis and trend monitoring.

  - The study established guidelines for future data collection using the Iowa Data Bike, including optimal image capturing intervals and camera angles to maximize the detection of surface distresses.

  - Based on the optimal image capturing interval of 2 seconds, image frequency issues on the network-level data ensured refined datasets.

In conclusion, the integration of smartphone-based roughness evaluation and deep learning-based distress detection provides a robust framework for trail management. This approach not only enhances the accuracy and efficiency of trail condition assessments but also supports proactive maintenance planning, ensuring the safety and quality of recreational pathways in Central Iowa. Further refinement and validation of these methods will continue to improve the reliability and applicability of the system in various trail management scenarios.

REFERENCES

Ahlin, K., and Granlund, N. O. J. (2002). Relating road roughness and vehicle speeds to human whole body vibration and exposure limits. International Journal of Pavement Engineering, 3(4), 207–216.

Alatoom, Y. I., and Obaidat, T. I. (2021). Measurement of street pavement roughness in urban areas using smartphone. International Journal of Pavement Research and Technology, 15(4), 1003–1020. https://doi.org/10.1007/s42947-021-00069-3

Alatoom, Y. I., and Obaidat, T. I. (2022). Development of pavement roughness models using artificial neural network (ANN). International Journal of Pavement Engineering, 23(13), 4622–4637. https://doi.org/10.1080/10298436.2021.1968396

Alatoom, Y. I., Zihan, Z. U., Nlenanya, I., Al-Hamdan, A. B., and Smadi, O. (2024). A sequence-based hybrid ensemble approach for estimating trail pavement roughness using smartphone and bicycle data. *Infrastructures*, 9(10), 179. https://doi.org/10.3390/infrastructures9100179.

AASHTO. (2012). Guide for the development of bicycle facilities (4th ed.). American Association of State Highway and Transportation Officials.

Arora, M. K., Patel, M. R., and Titiksh, A. (2021). Study of pavement unevenness using sensor-based smartphone software. In K. K. Pathak, J. M. S. Jaya, A. R. Bandara, and A. R. Pathak (Eds.), Recent trends in civil engineering (pp. 879–898). Springer Singapore.

ARRB Group Ltd. (2017) User Manual: Walking Profiler G3. Issue date 06 September.

Attard, L., Debono, C. J., Valentino, G., Di Castro, M., Masi, A., and Scibile, L. (2019). Automatic crack detection using mask R-CNN. 2019 11th international symposium on image and signal processing and analysis (ISPA),

Bíl, M., Andrášik, R., and Kubeček, J. (2015). How comfortable are your cycling tracks? A new method for objective bicycle vibration measurement. Transportation Research Part C: Emerging Technologies, 56, 415–425. https://doi.org/10.1016/j.trc.2015.04.017

Cafiso, S., di Graziano, A., Marchetta, V., and Pappalardo, G. (2022). Urban road pavements monitoring and assessment using bike and e-scooter as probe vehicles. Case Studies in Construction Materials, 16, e00889.

Chou, C.-P., Siao, G.-J., Chen, A.-C., and Lee, C.-C. (2020). Algorithm for estimating International Roughness Index by response-based measuring device. Journal of Transportation Engineering, Part B: Pavements, 146(3), 04020031.

Des Moines Area MPO. (2018). Central Iowa Trail Condition: 2018 Report.

Des Moines Area MPO. (2019). Central Iowa Trail Condition: 2019 Report.

Des Moines Area MPO. (2023). Des Moines Area MPO. https://dmampo.org/

Ghosh, R., and Smadi, O. (2021). Automated detection and classification of pavement distresses using 3D pavement surface images and deep learning. Transportation Research Record, 2675(9), 1359-1374.

Haque, M. A. (2022). Feature engineering and selection for explainable models: A second course for data scientists. Lulu Press, Inc.

He, K., Gkioxari, G., Dollár, P., and Girshick, R. (2017). Mask R-Cnn. Proceedings of the IEEE international conference on computer vision,

Hoang, N.-D. (2018). Detection of surface crack in building structures using image processing technique with an improved Otsu method for image thresholding. Advances in Civil Engineering, 2018.

Hosseini, S. A., and Smadi, O. (2021). How prediction accuracy can affect the decision-making process in pavement management system. Infrastructures, 6(2), 28. https://doi.org/10.3390/infrastructures6020028

Hsieh, Y.-A., and Tsai, Y. J. (2020). Machine learning for crack detection: Review and model performance comparison. Journal of Computing in Civil Engineering, 34(5), 04020038.

Ibragimov, E., Kim, Y., Lee, J. H., Cho, J., and Lee, J.-J. (2024). Automated Pavement Condition Index Assessment with Deep Learning and Image Analysis: An End-to-End Approach. Sensors, 24(7), 2333.

International Organization for Standardization. (1997). ISO 2631-1: Mechanical vibration and shock — Evaluation of human exposure to whole-body vibration — Part 1: General requirements (2nd ed.). ISO.

Janani, L., Doley, R., Sunitha, V., and Mathew, S. (2022). Precision enhancement of smartphone sensor-based pavement roughness estimation by standardizing host vehicle speed. Canadian Journal of Civil Engineering, 49(5), 716–730.

Jia, X., Huang, B., Zhu, D., Dong, Q., and Woods, M. (2018). Influence of measurement variability of International Roughness Index on uncertainty of network-level pavement evaluation. Journal of Transportation Engineering, Part B: Pavements, 144(2), 04018007.

Landis, B. W., Petritsch, T. A., Huang, H. F., and Do, A. H. (2004). Characteristics of emerging road and trail users and their safety. Transportation Research Record: Journal of the Transportation Research Board, 1878(1), 131–139. https://doi.org/10.3141/1878-17

Levenberg, K. (1944). A method for the solution of certain nonlinear problems in least squares. Quarterly of Applied Mathematics, 2(2), 164–168.

Loprencipe, G., Zoccali, P., and Cantisani, G. (2019). Effects of vehicular speed on the assessment of pavement road roughness. Applied Sciences, 9(9), 1783.

Ma, C., Chen, Y., and Zhang, Y. (2021). Simulation analysis of the evolution of sustainable operation of transport infrastructure projects under government regulation based on prospect theory and BP neural network. Scientific Programming, 2021(1), 6868487.

Mathavan, S., Vaheesan, K., Kumar, A., Chandrakumar, C., Kamal, K., Rahman, M., and Stonecliffe-Jones, M. (2017). Detection of pavement cracks using tiled fuzzy Hough transform. Journal of Electronic Imaging, 26(5), 053008-053008.

Mei, Q., and Gül, M. (2020). A cost effective solution for pavement crack inspection using cameras and deep neural networks. Construction and Building Materials, 256, 119397.

Múčka, P. (2017). International Roughness Index specifications around the world. Road Materials and Pavement Design, 18(4), 929–965.

Niska, A. M., Sjögren, L., Weber, C., De Jong, T., and Fyhri, A. (2022). Determination of riding comfort on cycleways using a smartphone app [SSRN Electronic Journal].

Obaidat, T. I. A., and Alatoom, Y. I. (2022). Development of pavement roughness regression models based on smartphone measurements. Journal of Engineering, Design and Technology, 4, 1136–1157. https://doi.org/10.1108/jedt-12-2021-0723

Podder, S., Bhattacharjee, S., and Roy, A. (2021). An efficient method of detection of COVID-19 using Mask R-CNN on chest X-Ray images. AIMS Biophys, 8(3), 281-290.

Qureshi, W. S., Hassan, S. I., McKeever, S., Power, D., Mulry, B., Feighan, K., and O'Sullivan, D. (2022). An exploration of recent intelligent image analysis techniques for visual pavement surface condition assessment. Sensors, 22(22), 9019.

Sandamal, R. M. K., and Pasindu, H. R. (2022). Applicability of smartphone-based roughness data for rural road pavement condition evaluation. International Journal of Pavement Engineering, 23(3), 663–672.
Sayers, M. W. (1986). The international road roughness experiment: Establishing correlation and a calibration standard for measurements (Report No. UMTRI-86-04). University of Michigan Transportation Research Institute.
Sellami, E. M., and Rhinane, H. (2024). A modern method for building damage evaluation using deep learning approach-Case study: Flash flooding in Derna, Libya. E3S Web of Conferences.
Shtayat, A., Moridpour, S., Best, B., and Rumi, M. S. (2020). Using a smartphone software and a regular bicycle to monitor pavement health status. In Proceedings of the 2020 2nd International Conference on Robotics Systems and Vehicle Technology (pp. 121–126). Association for Computing Machinery.
Šimun[1], M., and Rukavina, T. (2010) Roughness of The Motorway Driving Surface. First International Conference on Road and Rail Infrastructure. Opatija, Croatia.
Sjölander, A., Belloni, V., Ansell, A., and Nordström, E. (2023). Towards automated inspections of tunnels: A review of optical inspections and autonomous assessment of concrete tunnel linings. Sensors, 23(6), 3189.
Titov, W., and Schlegel, T. (2019). Monitoring road surface conditions for bicycles – Using mobile device sensor data from crowd sourcing. In H. Krömker (Ed.), HCI in mobility, transport, and automotive systems (pp. 340–356). Springer International Publishing.
Uddin, W., Hudson, W. R., and Elkins, G. (1990). Surface-smoothness evaluation and specifications for flexible pavements. ASTM Special Technical Publication, (1031), 224–236.
Uwizera, D. K., Ruranga, C., and McSharry, P. (2022). Deep Learning Inter-city Road Conditions in East Africa Focusing on Rwanda for Infrastructure Prioritization using Satellite Imagery and Mobile Data. SAIEE Africa Research Journal, 114(1), 14-24.
Wage, O., Feuerhake, U., Koetsier, C., Ponick, A., Schild, N., Beening, T., and Dare, S. (2020). Ride vibrations: Towards comfort-based bicycle navigation. The International Archives of the Photogrammetry, Remote Sensing and Spatial Information Sciences, XLIII-B4-2020, 367–373.
Yamashita, R., Nishio, M., Do, R. K. G., and Togashi, K. (2018). Convolutional neural networks: an overview and application in radiology. Insights into imaging, 9, 611-629.
Yang, X., Hu, L., Ahmed, H. U., Bridgelall, R., and Huang, Y. (2022). Calibration of smartphone sensors to evaluate the ride quality of paved and unpaved roads. International Journal of Pavement Engineering, 23(5), 1529–1539
Yu, Q., Fang, Y., and Wix, R. (2022). Pavement roughness index estimation and anomaly detection using smartphones. Automation in Construction, 141, 104409
Zang, K., Shen, J., Huang, H., Wan, M., and Shi, J. (2018). Assessing and mapping of road surface roughness based on GPS and accelerometer sensors on bicycle-mounted smartphones. Sensors, 18(3), 914.
Zhang, Z., Zhang, H., Xu, S., and Lv, W. (2022). Pavement roughness evaluation method based on the theoretical relationship between acceleration measured by smartphone and IRI. International Journal of Pavement Engineering, 23(9), 3082–3098

Zihan, Z. U., Smadi, O., Tilberg, M., and Yamany, M. S. (2023). Synthesizing the performance of deep learning in vision-based pavement distress detection. Innovative Infrastructure Solutions, 8(11), 299.

APPENDIX A. QUALITY CONTROL PLAN FOR TRAIL MANAGEMENT PROGRAM – DES MOINES AREA METROPOLITAN PLANNING ORGANIZATION

A.1. Introduction

The purpose of this Quality Control (QC) Plan is to establish a systematic approach for ensuring the accuracy, consistency, and reliability of data collected through the Trail Management Program by the Des Moines Area Metropolitan Planning Organization (MPO). By defining quality control procedures across data collection, processing, and analysis workflows, this plan supports high-confidence decision-making related to trail maintenance, rehabilitation, and long-term asset management.

The Trail Management Program is designed to evaluate the condition of paved trails using a combination of mobile sensor platforms and advanced analytics. A customized bicycle-based data collection system, referred to as the Iowa Data Bike, captures georeferenced images and vertical acceleration data, enabling the estimation of trail roughness through the Bike Roughness Index (BRI). In parallel, high-resolution trail imagery is used to detect and quantify surface distresses through a deep learning-based instance segmentation model. These components provide a scalable, data-driven method for assessing trail conditions across the regional network.

This QC Plan ensures that each stage of the program, ranging from field deployment and sensor calibration to image analysis and geographic information systems (GIS) integration, follows established protocols for quality control and verification. It also defines roles and responsibilities, corrective action steps, and continuous improvement practices to maintain data integrity and support trail management objectives over time.

A.2. Trail Management Program Overview

The Trail Management Program was developed to establish a scalable and objective framework for evaluating the condition of paved trails throughout the Des Moines metropolitan area. The main goal is to support proactive maintenance and capital planning by providing detailed, quantitative insights into surface roughness and visible trail distresses. By combining dynamic sensing technologies with automated image analysis and GIS-based visualization, the program enables network-wide assessment of trail conditions in a cost-effective and repeatable manner.

Key components include the following:

- **Iowa Data Bike**: The Iowa Data Bike, developed and built by the Des Moines Area MPO in 2017, is a bicycle equipped with an iPhone (used to record vertical motion data) and a GoPro camera mounted on the back of the bike for capturing geotagged trail surface imagery. This platform allows for flexible, non-intrusive data collection along paved trails, capturing both ride quality and visual surface features.

- **BRI estimation**: Vertical motion data recorded from the iPhone is processed to compute the BRI, a metric for assessing surface roughness. The index is calculated through a double integration and RMS-based method analyzing acceleration signals, filtered and segmented by Global Positioning System (GPS)-based distance intervals (typically 0.3 mi), providing a repeatable metric that correlates with standard roughness indices obtained by the Class 1 profiler.
- **Vision-based distress detection using Mask R-CNN**: Trail surface images collected by the Iowa Data Bike are analyzed using a deep learning-based instance segmentation model (e.g., Mask R-CNN). The model was trained to identify and delineate eight types of trail surface distresses. The model enables automated detection, localization, and quantification of the surface distress extent. The system provides a consistent measure of surface defects while reducing the need for manual interpretation.
- **GIS integration and network-level management**: All the condition metrics calculated for trail assessment are georeferenced and integrated into a GIS environment, allowing for spatial visualization and analysis at the trail segment and system levels. The output includes trail condition maps supporting segment-level summary tables, time-series comparisons, data-driven prioritization, and long-term trail maintenance planning.

A.3. QC Objectives and Strategy

The QC strategy for the Trail Management Program is designed to ensure the reliability, repeatability, and validity of data collected across all trail segments. As the program integrates sensor-based roughness measurements and vision-based surface distress detection, robust QC practices are essential for maintaining confidence in the data and the insights derived from them.

The core objectives of this QC Plan are as follows:

- Guarantee consistent and accurate data collection through standardized field and processing protocols
- Minimize errors and data loss during acquisition, transfer, and analysis
- Enable reproducible results across years and trail networks
- Support continuous improvement through structured feedback and corrective action mechanisms

To meet these objectives, the QC framework is organized around several key quality management categories:

- **Equipment calibration and certification**: All sensors and data collection devices, including the iPhone accelerometer and GoPro camera, are subject to routine calibration procedures to ensure accurate measurements. Mounting positions, device alignment, and data logging settings are verified before each field session.
- **Personnel training**: Team members involved in data collection and distress annotation for future model training should receive formal training and be provided with standard operating procedures (SOPs).

- **Pre-collection checks**: Prior to each data collection cycle, verification of GPS functionality, storage capacity, battery levels, and camera framing is conducted. Standard test runs are used to validate accelerometer output and trail coverage.
- **In-field and post-collection quality assurance**: Data is reviewed immediately after collection to identify missing geotags, blurry images, or irregular sensor signals. Roughness profiles and sample imagery are checked for anomalies before proceeding to batch processing. When applicable, automated QC scripts are used to filter out incomplete, redundant, or low-quality data points.
- **Error handling and corrective actions**: QC thresholds are defined for acceptable variability in the BRI and image-based distress predictions. If deviations exceed these thresholds, the affected segment is flagged for review and, if necessary, re-collection. All corrective actions are logged with explanations and resolutions to support accountability and continuous improvement.

The program employs an annual control site strategy. These designated trail segments serve as benchmarking anchors to assess long-term consistency in equipment performance, field procedures, and model outputs.

- **Annual control sites**: These high-confidence reference segments are surveyed once per year and include previously validated BRI and surface distress data. They are used to benchmark sensor calibration, evaluate long-term drift, and verify model consistency across years and trail types.

The timing and scope of QC activities throughout the program lifecycle are illustrated in Figure A.1, which aligns core quality assurance (QA) tasks with the phases of data collection. This timeline ensures that the early calibration, rigorous setup, and post-collection review stages are executed with consistency.

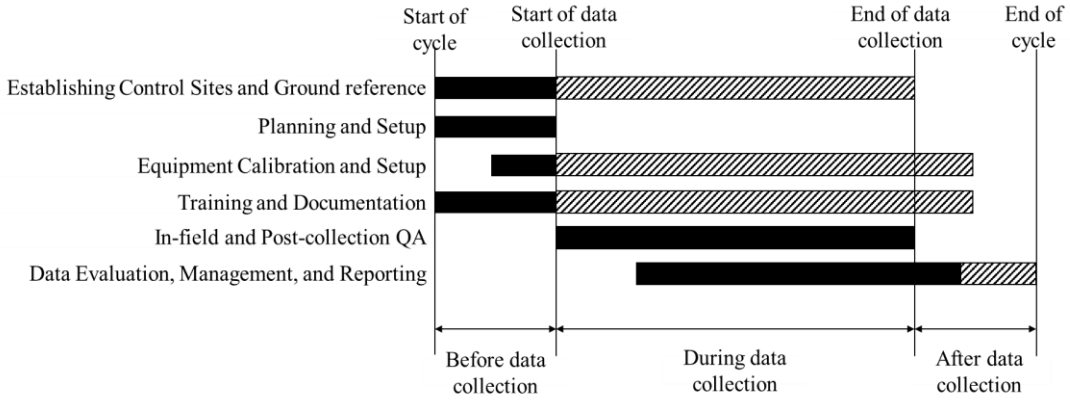


Figure A.1. Temporal alignment of QA activities relative to the data collection cycle

A.4. Equipment Calibration and Setup

Reliable and consistent data collection is fundamental to the Trail Management Program. This section outlines the sensors and devices used for data collection, the calibration procedures required to ensure their accuracy, and the role of designated control segments in validating system performance throughout the data collection cycle.

A.4.1. Sensors and Equipment Used

The Iowa Data Bike is equipped with the following components for synchronized roughness and imagery data collection:

- **iPhone accelerometer**: Used to capture vertical acceleration data, which serves as the input for calculating the BRI. The iPhone utilizes the SensorLog app to record acceleration data along the X, Y, and Z axes, along with general logging information such as timestamps, GPS coordinates, and bike speed. The app operates with a minimum sampling frequency of 100 Hz. In addition to linear acceleration, SensorLog may also collect other motion-related data such as gyroscope and magnetometer readings.
- **Camera sensor**: Mounted on the rear of the bike, the camera is configured to capture high-resolution trail surface imagery at intervals of at least every 2 seconds. The program uses a GoPro Hero 10 Black, which features a 23 megapixel sensor and is set to a wide-angle field of view to capture the entire trail width. Additional internal settings and configurations are provided in Table A.1.
- **GPS Logging**: GPS data is recorded to ensure the geotagging of each image and associate acceleration signals with trail locations. Accurate location referencing is critical for segment-level analysis and GIS integration.

Table A.1. Detailed camera settings used for trail data collection

Settings	Recommended Camera Settings
Image Height	5568
Image Width	4176
Horizontal Resolution	72
Vertical Resolution	72
Color representation	--
Camera maker	GoPro
Camera model	HERO10 Black
F-stop	f/2.5
Exposure time	1/964 sec.
ISO Speed	ISO-101
Exposure bias	0 step
Focal length	3 mm
Max aperture	2.5
Metering mode	Average
Flash mode	No flash function
35mm focal length	15
Contrast	Normal
Light Source	Daylight
Exposure program	Normal
Saturation	High Saturation
Sharpness	Normal
White balance	Auto
Digital zoom	1
EXIF version	0221

A.4.2. Calibration Procedures

To ensure consistent sensor performance and reduce error propagation, the following calibration protocols are implemented before each field deployment:

- **Accelerometer calibration**: A baseline calibration of the iPhone's accelerometer is performed before data collection by placing the device on a stationary, level surface and capturing reference data to verify zero-acceleration conditions. Any drift is addressed before proceeding.
- **Camera mount standardization:** The GoPro camera is mounted at a predetermined height and angle to ensure a consistent field of view across all data collection sessions. It is securely fastened using a standardized bracket that maintains a fixed orientation relative to the bike or collection platform. This setup minimizes variability in image perspective, alignment, and coverage, which is critical for ensuring uniformity in surface distress detection and enabling reliable comparisons between different trail segments or time periods. A calibration image is captured prior to each ride to confirm alignment with the trail surface and ensure consistent framing across sessions.
- **GPS verification:** Before data collection, GPS signal strength and accuracy are checked on both the smartphone and the camera system to ensure a positional accuracy of at least 3 meters. If either device shows weak GPS reception, such as in wooded or obstructed areas,

alternate collection routes or buffer zones are planned to prevent gaps or errors in georeferencing.

A.4.3. Control Segments

To assess and maintain the integrity of sensor outputs, the program designates specific trail segments as **control sites**:

- **Annual Control Sites**: These are carefully selected trail segments of a specified length (e.g., 0.3 mi) that are revisited once a year and have previously documented roughness levels and surface distress types. They are chosen to represent a range of pavement surface types (e.g., asphalt and concrete), cover different geographic areas across the network, and include a variety of condition states (e.g., excellent to poor). These sites serve as reference points to verify sensor calibration, ensure consistency in BRI calculations, and evaluate the accuracy and stability of the image-based distress detection models over time.

A.5. Data Collection Quality Control

Consistent and accurate data collection is essential to ensure that the outputs of the Trail Management Program are reliable and actionable. This section outlines the SOPs followed during fieldwork, along with specific quality control measures applied to both imagery and accelerometer data. These protocols are designed to reduce noise, eliminate unusable data, and enhance the repeatability of trail condition assessments.

A.5.1. Standard Operating Procedures

To maintain consistency across data collection efforts, the following procedures are applied during each field deployment:

- The rider maintains a **consistent speed of 7 to 8 mph** during collection. This speed ensures optimal data resolution and stability for both image capture and vertical acceleration logging.
- Trail segments are divided and analyzed in sections with a **minimum length of 0.3 mi**, providing sufficient data points for localized condition evaluation without sacrificing spatial resolution.
- To ensure consistent framing and field of view in the collected images, the rider follows a centered path, riding in the middle of the lane whenever possible. This positioning facilitates optimal camera alignment and minimizes distortion due to edge effects or uneven pavement features.

A.5.2. Image Quality Checks

High-resolution images captured during each ride are subjected to multiple quality control steps to ensure they are suitable for automated distress detection:

- Images are captured at a **2-second time-lapse interval**, which balances coverage density with data storage efficiency.
- Image Orientation Verification: All images are automatically checked for proper orientation using EXIF metadata and visual validation protocols. Images that are rotated incorrectly (e.g., upside down, sideways) are either automatically corrected using EXIF orientation tags or flagged for manual review. This step ensures consistent image orientation before feeding data into the deep learning model, preventing detection errors caused by unexpected viewing angles.
- Post-processing includes the **filtering of blurry, redundant, or overexposed images,** using both automated image quality metrics and manual review when needed.
- Each image is **validated for GPS geotagging accuracy** and its spatial alignment with the planned trail route (shapefile). Images without proper geolocation data or those deviating from the mapped route are flagged and may be excluded from further analysis.

A.5.3. Accelerometer Data QA

Vertical acceleration data collected via the iPhone accelerometer is the basis for calculating the BRI. To ensure valid and interpretable BRI values, the following quality control checks are performed:

- **Outlier filtering** is applied to remove anomalous acceleration spikes that may result from sudden braking, potholes not representative of general trail condition, or GPS errors. The filtering is based on the root mean square (RMS) of vertical acceleration within each segment.
- **Speed filtering** is implemented to remove data captured during stops or very low-speed travel. Any data recorded while the bike is moving at **less than 1 mph** is excluded from BRI calculation to prevent skewed results.
- **Thresholding and smoothing** techniques are applied during BRI computation to stabilize the output and minimize the effects of short-term anomalies. A rolling window approach is used to calculate BRI values at the segment level, ensuring continuity across the network.

A.5.4. Data Quality Assessment and Outlier Detection

To ensure the reliability and consistency of both roughness and distress measurements, an automated outlier detection methodology is implemented as part of the data processing pipeline. This systematic approach identifies and flags extreme values that may result from equipment malfunctions, environmental anomalies, measurement errors, or processing inconsistencies during automated analysis.

A.5.4.1. Outlier Detection Methodology

The program employs the interquartile range (IQR) method for outlier identification across all distress measurement categories and roughness metrics. The IQR method is selected for its

robustness to non-normal data distributions and its effectiveness in identifying extreme values without making assumptions about the underlying data characteristics.

The outlier detection algorithm operates as follows:

- Calculate the first quartile (Q1), third quartile (Q3), and interquartile range (IQR = Q3 - Q1) for each measurement category.
- Establish outlier boundaries using a configurable IQR multiplier (typically 2.0 for conservative detection).
- Flag measurements that fall outside the bounds of Q1 - (multiplier × IQR) and Q3 + (multiplier × IQR).
- Process each distress category independently to account for varying measurement ranges and distribution characteristics.

A.5.4.2. Application Scope

The outlier detection process is applied to the following:

- All nine distress measurement categories from automated detection (interconnected cracking, longitudinal cracking, object detection, patching, pothole, sealed longitudinal cracking, spalling, T-joints, and transverse cracks)
- BRI values calculated from accelerometer data
- Derived metrics such as distress density, crack intensity, and area measurements

A.5.4.3. Quality Thresholds and Action Triggers

Data retention rates below 95% for any individual measurement category trigger a review of collection procedures, equipment calibration, or model performance. Segments with multiple outlier flags across different distress types are prioritized for manual verification or re-collection to ensure data reliability.

This systematic approach to outlier detection enhances data quality by removing anomalous measurements while preserving legitimate high-distress readings that may indicate critical maintenance needs, thereby supporting confident decision-making in trail management and maintenance planning.

Together, these procedures help maintain a high level of data quality and integrity, ensuring that both roughness and distress metrics accurately reflect true trail surface conditions.

A.6. Ground Reference and Validation

To evaluate the accuracy of the BRI and ensure consistency in trail condition measurements, a validation framework has been established using ground reference data from walking profilers. These high-precision devices serve as a benchmark for comparing accelerometer-derived roughness estimates, allowing for quantitative validation of the BRI methodology.

A.6.1. Reference Trails

The control segments will be designated as reference trails based on the availability of previously collected walking profiler data. These segments represent a range of surface conditions and are revisited periodically to support calibration and performance evaluation of the BRI estimation process.

A.6.2. Validation Metrics

To assess the agreement between BRI and the reference International Roughness Index (IRI) values collected via walking profilers, the following validation metrics are used:

- **Root mean square error (RMSE):** RMSE is calculated between BRI and the corresponding IRI values from walking profiler data for each matched segment. This metric quantifies the average deviation of the BRI estimates from the reference measurements.
- **Correlation coefficient (R^2):** The strength of the linear relationship between BRI and IRI is evaluated using the coefficient of determination (R^2). A **minimum threshold of 0.75** is used to indicate acceptable agreement and model reliability.
- **Maximum allowable RMSE:** For a segment to pass validation, the BRI-to-IRI comparison must result in an RMSE **no greater than 100 in./mi**. Exceeding this threshold prompts a review of calibration settings or field data quality.

These validation procedures ensure that the BRI remains a dependable surrogate for rider-perceived surface roughness and that the data collected through the Trail Management Program is consistent with industry-accepted roughness evaluation standards.

A.7. Automated Distress Detection QA

A key feature of the Trail Management Program is the automated detection of surface distresses using a deep learning–based instance segmentation model (Mask R-CNN). To ensure reliable and interpretable outputs, a structured QA process supports all stages of the pipeline—from annotation to prediction evaluation and measurement refinement.

Although a trained model has already been deployed for network-level inference, the QA plan allows for iterative improvements over time. Future model retraining can be supported by expanding the training dataset, especially with new or underrepresented distress types. Model

evaluation is conducted annually on designated control trail segments. When necessary, ground truth can be collected using unmanned aerial vehicle (UAV) imagery, field tapes, or manual measurements to validate and refine distress quantification scales.

Key QA activities include the following:

- Manual polygon annotations are developed for eight distress classes (e.g., longitudinal cracking, transverse joints, spalling, patching).
- Dataset split follows a strict train-validation separation to prevent performance bias.
- A minimum mAP of 0.50 is required for model deployment; overfitting is monitored via validation loss trends.
- Post-processing includes Intersection over Union (IoU) filtering and distress category prioritization to reduce redundant or overlapping predictions.
- Predicted length, area, and count of distresses are computed and used for trail- and network-level condition summaries.
- Real-world scaling is calibrated using taped reference markers and validated nonlinear models to convert pixel-level predictions into actual dimensions.
- When inconsistencies are observed, especially in annual control segments, the scaling model may be adjusted to reflect improved accuracy in measurement translation.

This QA framework ensures that automated trail surface assessments are not only robust and scalable but also grounded in repeatable field-verified procedures.

A.8. GIS and Data Management QA

Effective data management is critical for ensuring the long-term usability, and accuracy of trail condition information generated through the Trail Management Program. All outputs from the roughness and distress detection pipelines are integrated into a GIS environment, which supports visualization, analysis, and reporting at the segment level. This section outlines the quality assurance procedures applied to ensure the integrity and completeness of GIS data.

A.8.1. Segment ID Assignment

A unique trail segment ID is assigned to each continuous stretch of trail data, typically segmented at 0.3 mi intervals or logical breaks in geometry. This ID enables efficient aggregation of distress and roughness data at the segment level and simplifies network-wide summaries, trend analysis, and maintenance planning.

A.8.2. Attribute Completeness

For **segment-level summaries**, particularly for planning and reporting, the following attributes must also be computed and included:

- **ParkID**: Unique identifier for the trail segment
- **StartX/StartY and EndX/EndY**: Coordinates marking the beginning and end of the trail segment
- **Distress Type**: Categorical label (e.g., longitudinal crack, patching, spalling)
- **Distress Count**: Number of instances detected for each distress type (e.g., patching, spalling)
- **Distress Length (ft)**: Total linear extent of line-based distresses (e.g., cracks)
- **Distress Area (ft^2)**: Total area affected by surface-level distresses (e.g., interconnected cracking)
- **BRI**: Bike Roughness Index averaged across the segment
- **Year**: Calendar year of data collection

These attributes are essential for enabling meaningful comparison across trail segments and over time.

A.8.3. Data Backup and Versioning

All processed outputs and intermediate datasets—including GIS shapefiles, raw and filtered image sets, and roughness summaries—are backed up in a version-controlled environment. Each dataset is tagged with a date-stamped version identifier to track revisions, support reproducibility, and allow rollbacks if errors are discovered. Metadata logs accompany each version to document processing parameters and known data issues.

These GIS and data management QA procedures help maintain the quality, accessibility, and auditability of the Trail Management Program's growing spatial dataset.

A.9. Corrective Actions and Error Resolution

Despite rigorous quality control procedures, occasional data inconsistencies, equipment malfunctions, or model performance issues may arise during the trail assessment process. To ensure data integrity and maintain confidence in the outputs, the Trail Management Program includes a defined protocol for identifying, reviewing, and resolving such issues through structured corrective actions.

A.9.1. Thresholds for Triggering Review

Specific thresholds should be established to flag potential issues that warrant further investigation:

- Significant deviations in BRI values compared to historical records for the same trail segment (e.g., deviations exceeding 50 IRI in./mi)
- Incomplete attributes or poor-quality images affecting a substantial portion of a trail segment (e.g., more than 10% of images)

- Automated distress predictions with large discrepancies in segmented area when compared to a validated ground reference (e.g., greater than 20% error)

When any of these conditions are met, a review process is initiated to assess whether the issue stems from data anomalies, processing errors, or equipment-related faults.

A.9.2. Corrective Action Steps

The following steps are taken when an error or inconsistency is confirmed:

- The issue is **flagged and documented in the QC log**, including details on the segment affected, nature of the error, and the triggering threshold exceeded
- A targeted **re-annotation** of images or **re-collection** of field data is conducted, depending on the source of the issue
- All corrective actions and final outcomes are **thoroughly documented**, including the resolution date, responsible personnel, and any follow-up steps required

This process ensures a transparent record of quality issues and responses while enabling continuous improvement in field practices, annotation protocols, and model development. Over time, recurring issues can be analyzed to refine QA thresholds and improve training and calibration standards.

A.10. Training and Documentation

Effective quality control depends not only on sound procedures and tools but also on a well-trained team that understands and consistently applies them. The Trail Management Program incorporates structured training and documentation practices to ensure consistency, reduce human error, and support long-term program sustainability.

A.10.1. Annotation Team Training

All annotation personnel involved in labeling trail surface distresses are trained using **predefined distress labeling guidelines.** These guidelines include clear definitions, visual examples, and polygon-drawing protocols for each of the target distress types. Emphasis is placed on annotation consistency and adherence to masking standards.

A.10.2. Annual Refresher Training

Each year, all team members involved in data collection, processing, and analysis receive a **refresher training** covering key aspects of the program's technical workflows. This training ensures that staff are up to date on protocols and familiar with any updates or enhancements to tools and procedures. The refresher includes:

- **Camera and accelerometer setup**: Procedures for consistent sensor calibration, mounting configuration, and operational checks before each ride.
- **Data processing pipeline**: Step-by-step walkthrough of the workflows used to transform raw data into actionable trail condition metrics, including accelerometer filtering, BRI calculation, image preprocessing, model inference, and post-processing.
- **QC protocols and error handling**: Review of QA/QC checkpoints, error detection thresholds, and corrective action steps across the entire data lifecycle—from field acquisition to GIS integration.

A.10.3. Training Documentation and Logs

To ensure transparency and accountability, detailed **training logs** are maintained. These records document:

- Dates and topics of each training session
- Names and roles of attendees
- Trainers or facilitators involved
- Completion of hands-on tasks or knowledge assessments
- Any corrective actions or retraining required

These logs not only support internal audits and quality reviews but also ensure that the program can onboard new team members efficiently while preserving institutional knowledge.

A.11. Reporting and Continuous Improvement

An effective QC Plan not only addresses the detection and resolution of data issues but also promotes transparency, accountability, and continual enhancement of methodologies over time. The Trail Management Program incorporates a structured reporting and feedback loop to evaluate progress, monitor performance, and support long-term improvements in data collection and analysis.

A.11.1. Quarterly Reporting

At the end of each quarter, a summary report is prepared to document the program's activities and highlight key quality control findings. These reports serve as internal audits and communication tools for project stakeholders. Each report includes the following:

- **Trail segments assessed**: A list of all parks and trail segments covered during the reporting period, including total distance evaluated and number of data runs.
- **QA findings and flagged issues**: A summary of quality assurance checks, including any thresholds exceeded, duplicate records identified, or image/sensor anomalies detected.

- **Corrective actions taken**: A record of all issues resolved during the quarter, including re-collections, re-annotations, and model updates. The log includes segment IDs, resolution steps, and responsible personnel.
- **Model retraining and improvements**: Updates on any changes made to the Mask R-CNN model, including retraining with new annotations, changes in data augmentation, or performance improvements based on mAP or validation loss metrics.

These reports are reviewed internally and can be shared with the MPO and partnering agencies as part of the program's commitment to transparency.

A.11.2. Annual SOP Updates

All SOPs related to data collection, processing, annotation, model evaluation, and GIS integration are reviewed and updated **annually**. This ensures alignment with current technologies, lessons learned, and field-tested improvements. Updates are logged with version numbers and effective dates to ensure traceability.

A.11.3. Stakeholder Feedback Implementation

Feedback from MPO stakeholders, partner agencies, reviewers, and field technicians is systematically collected and reviewed. This feedback is used to do the following:

- Refine SOPs and QA thresholds
- Update distress labeling guidelines
- Prioritize future model enhancements
- Inform the selection of control sites and validation segments

By embedding continuous improvement into both technical and operational workflows, the Trail Management Program ensures that its methods remain current, responsive, and aligned with the evolving needs of trail infrastructure planning and maintenance.

THE INSTITUTE FOR TRANSPORTATION IS THE FOCAL POINT FOR TRANSPORTATION AT IOWA STATE UNIVERSITY.

InTrans centers and programs perform transportation research and provide technology transfer services for government agencies and private companies;

InTrans contributes to Iowa State University and the College of Engineering's educational programs for transportation students and provides K–12 outreach; and

InTrans conducts local, regional, and national transportation services and continuing education programs.



IOWA STATE UNIVERSITY

Visit **InTrans.iastate.edu** for color pdfs of this and other research reports.